pipetting and 0.1% trypsin treatment, respectively. Then the cells were washed with PBS to remove the heparin and resuspended in 200 μL of StemSpan medium containing one of the cytokine cocktails that was used to prepare the concentrated viruses. These cell suspensions were then mixed with the concentrated viruses and overlaid on retronectin-coated wells (see above; 500 μL total volume/well of medium containing same cytokine cocktail). The cells were incubated at 37°C in 5% CO_2 for 3 days. Concentrated viruses (150 μL) were daily refurnished after the same volume of infection medium had been discarded. At the end of the 72-hour transduction, the floating and adherent cells were collected and GFP-positive cells were sorted and used for competitive and noncompetitive repopulation assays.

Retroviral transduction of the KSL cells was performed as previously described [12]. Briefly, 5×10^4 KSL cells were collected from 10 to 12 mice and seeded at a concentration of 1×10^4 in one retronectin-coated well of a 24-well dish and cultured in StemPro34 medium (Invitrogen) containing 50 ng/mL SCF, 20 ng/mL TPO, and 20 ng/mL FL in addition to the concentrated virus prepared in the same medium (MOI, 1.1–1.2 $\times 10^4$). Twenty-four hours after the culture, half of the medium was replaced with fresh concentrated virus and cultured for another 24 hours. After 48 hours the GFP-positive cells were sorted.

Noncompetitive repopulation assays

After sorting the GFP-positive cells from the FGF-1-expanded virus-transduced cells and from the virus-transduced KSL cells, we injected 1×10^5 and 1×10^3 cells, respectively, into a tail vein of 9.5 Gy irradiated B6-Ly5.2 recipient mice. Peripheral blood count and percentage of GFP-positive cells were evaluated every 2 weeks with FACS Calibur. Twelve weeks after the primary transplantation, the mice transplanted with FGF-1-expanded and virus-transduced cells were sacrificed, the GFP-positive cells from the BM were sorted, and 1×10^5 cells were injected into the B6-Ly5.2 secondary recipient after 9.5-Gy irradiation.

Competitive repopulating unit analysis

The experiment was performed on three cohorts of mice. In the first cohort, 2×10^5, 2×10^4, or 5×10^3 unfractionated fresh BM cells; in the second cohort, 1×10^5, 1×10^4, 3×10^3, 1×10^3, 3×10^2 3-week cultured cells in the presence of FGF-1; and in the third cohort, 1×10^5, 1×10^4 3×10^3, 1×10^3, 3×10^2 3-week cultured and then sorted retrovirus-transduced cells, respectively (individually designated as test cells) from B6-Ly5.1 mice were transplanted together with 2×10^5 competitor cells from Ly5.1/5.2 mice to 9.5 Gy irradiated B6-Ly5.2 recipients. Five to eight recipients were used in each arm. Ten weeks after transplantation, the proportion of the individual donor cells in the peripheral blood was determined using specific antibodies (see below). The animals were considered to be positive if >2% of both myeloid and lymphoid (B+T) cells were of donor origin 10 weeks after transplant. The frequency of the CRUs in the test cells was analyzed by Poisson statistics and the statistical software L-Calc (StemCell Technologies).

Flow cytometry

Flow cytometric analyses were performed on a FACS Calibur. The following antibodies were used: fluorescein isothiocyanate-CD45.2, phycoerythrin (PE)-Sca-1, PE-B220, PE-CD3, PE-CD45.1, allophycocyanate (APC)-c-kit, APC-CD4, APC-CD8, APC-CD45.2, peridinin chlorophyll protein (PerCp)-B220, PerCP-Cy5.5-CD45.2, and biotinylated CD45.1 and CD45.2. All antibodies were purchased from BD PharMingen (San Diego, CA, USA). The samples for staining were prepared by standard protocols. GFP fluorescence was detected using detector channel FL-1.

Results

Characterization of the BM cells cultured with FGF-1

We cultured unfractionated BM cells from B6-Ly5.1 mouse in heparin-supplemented serum-free medium in the presence of FGF-1 as a single cytokine, as described previously [6]. Cell numbers declined in the early phase of the culture, but after 2 weeks slowly started to increase. Most of the cells in the well at this time were nonadherent. As soon as small blast-like colonies loosely attached to the bottom appeared, the cells began expanding rapidly. We found that the percentage of Sca-1^+c-Kit^+ (KS) fraction gradually increased (0.13% and 11% after 1 and 2 weeks, respectively; data not shown) and reached the maximum of ~30% 3 weeks after culture initiation. In contrast, in BM cells cultured in the same medium but without FGF-1 and heparin, almost no KS cells were detected 3 weeks after the culture (Fig. 1A). We confirmed that 1×10^5 of unfractionated cells that had been grown in the presence of FGF-1 for 3 weeks conferred radiation resistance in the absence of rescue cells, and multilineage blood chimerism (>80% in myeloid and >50% in lymphoid populations) was observed in lethally irradiated congenic recipient mice at 3 months posttransplant (data not shown).

We also cultured unfractionated BM cells for 3 weeks in the same medium but in the presence of different cytokines or cytokine combinations such as 100 ng/mL SCF alone, 100 ng/mL SCF + 30 ng/mL TPO, or 100 ng/mL SCF + 30 ng/mL FGF-1. Interestingly, despite the fact that we detected similar ratios of KS cells in all of the above conditions, the percents of the donor-derived cell in the lethally irradiated recipients 3 months posttransplant in noncompetitive repopulation assays were about 10% and 5% in the myeloid and lymphoid populations, respectively (data not shown). Thus we concluded that only the cells cultured with FGF-1 alone potentially contain expanded HSCs that could be a target for retrovirus-mediated gene delivery.

Successful transduction of the FGF-1 expanded BM cells and characterization of the transduced cells

When we subjected FGF-1-cultured BM cells to the retrovirus transduction protocol in the presence of FGF-1 alone, the cells adhered to the bottom of the plate and slightly increased in number. Appearance of GFP-positive cells was very rare until 72 hours after transduction (data not shown). In contrast, in the presence of FGF-1 + SCF + TPO or SCF + TPO, most of the cells adhered to the bottom of the plate within 4 hours, and floating cells began to emerge on the

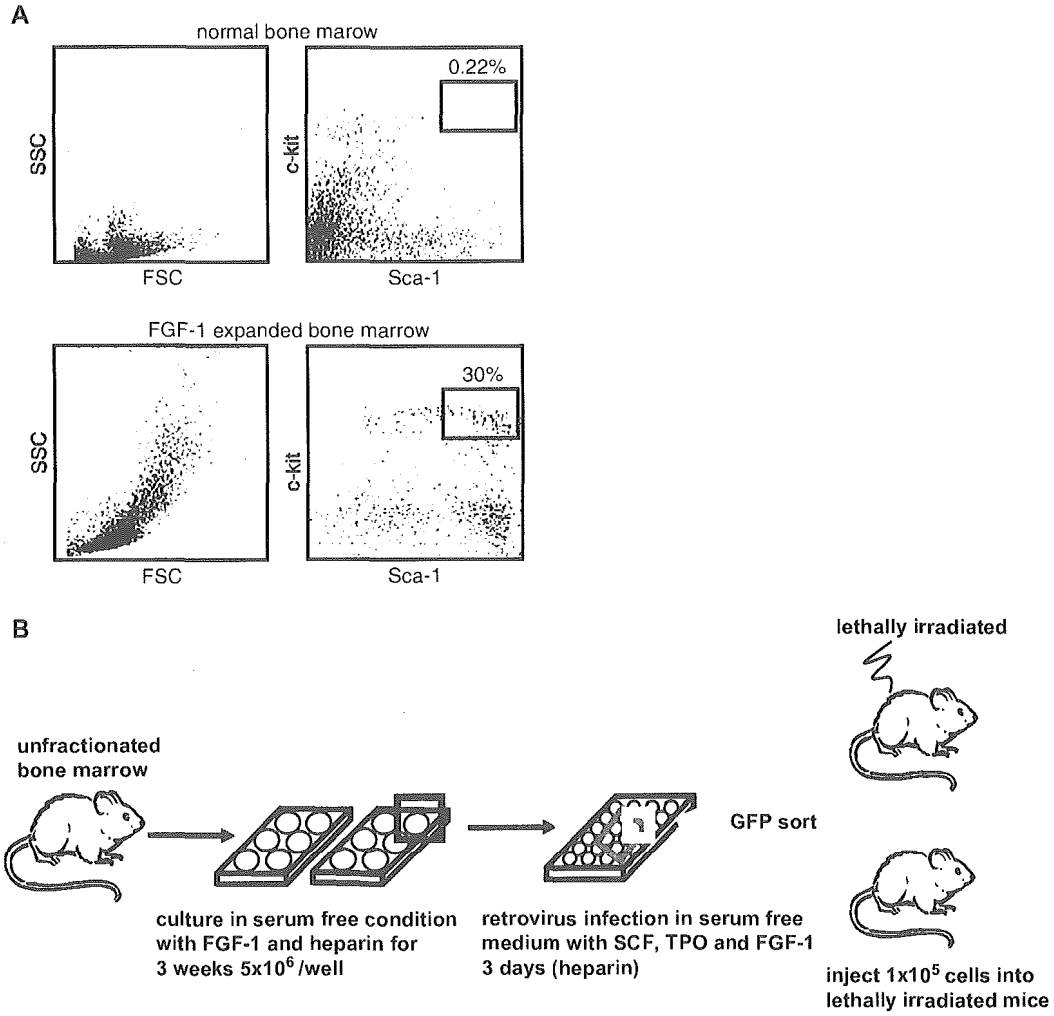

Figure 1. Characterization of BM cells cultured with FGF-1 and schematic representation of the method. **(A):** Unfractionated BM cells were cultured in the presence of FGF-1 and heparin. The cells cultured for 3 weeks showed highest percentage of $Sca1^+c\text{-}kit^+$ fraction (30%) and were used for the subsequent experiments. Cells cultured in the same conditions but without FGF-1 gave rise to almost no $Sca1^+c\text{-}kit^+$ cells. **(B):** Schematic representation of the experimental design. Unfractionated BM cells from a single mouse were cultured in two 6-well plates at a cell density of 5×10^6/well for a 3-week period with FGF-1 and heparin in serum-free medium. Both adherent and floating cells from one of these wells were then transferred to six wells of a 24-well plate and the transduction was performed as described in the Methods section. An average of 2×10^5 GFP-positive cells from each of these wells was sorted and injected into two lethally irradiated mice. For each recipient mouse, we used 1/150 of the cells from a single donor. Engraftment was achieved in 100% recipients.

next day and they then rapidly increased in number. Under the microscope, the majority of both floating and adherent cells were GFP-positive after 72 hours (Fig. 2A and data not shown).

By flow cytometric analyses, we confirmed much higher transduction efficiency when using the combinations of FGF-1 + SCF + TPO and SCF + TPO than FGF-1 alone during the transduction procedure (Fig. 2B). We observed that comparable ratios of $Sca1^+$ and $Sca1^-$ cells, and $c\text{-}Kit^+$ and $c\text{-}Kit^-$ cells were transduced with the combinations of FGF-1 + SCF + TPO and SCF + TPO (Fig. 2B). The percentage and absolute number of retrovirus-transduced KS cells were also greater when combinations of FGF-1 + SCF + TPO or SCF + TPO were chosen. Mudifewer KS cells were transduced in the presence of FGF-1 alone (Fig. 2B). The transduction efficiency was similar between the combinations of FGF-1 + SCF + TPO and SCF + TPO. The percentage of remaining KS cells, however, was slightly but consistently greater with the combination of FGF-1 + SCF + TPO (11 ± 1%) than with the combination of SCF + TPO (8 ± 0.8%; Fig. 2B). Thus, we decided to choose the former combination for our subsequent experiments. We sorted all the GFP-positive cells after a 3-week culture with FGF-1 alone and 3-day transduction with SCF + TPO + FGF-1. Interestingly, most of the GFP-positive cells in this condition were

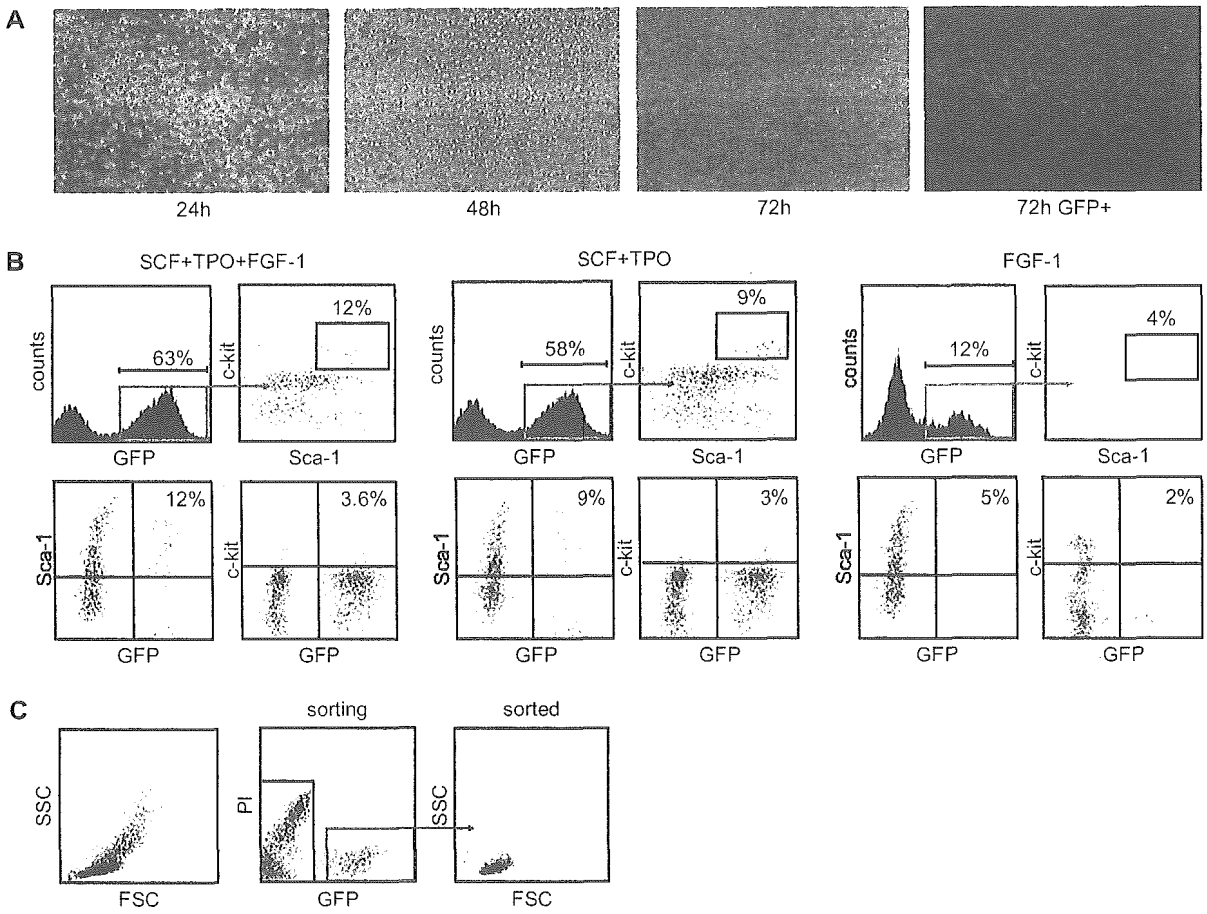

Figure 2. Successful transduction of the FGF-1-expanded BM cells. **(A):** Microscopic image of the cells during transduction procedure. Twenty-four hours after the transduction, almost all the cells attached to the bottom (left panel). The floating cells increased in number over the next 48 hours (second panel) and overgrew the adherent cells 72 hours (third panel) after commencing the transduction. Fluorescent microscopic observation showing GFP expression (right panel) is shown. Original magnification, ×40. **(B):** Optimization of the transduction protocol. After 3-week culture with FGF-1 and heparin, both adherent and nonadherent cells were transferred to fibronectin-coated dishes with medium containing the cytokines as previously described. These were subsequently transduced with virus supernatant from ψMP34 cells stably transduced with pMY/mock-11G retrovirus. Best results were obtained when using the combination of FGF-1, SCF, and TPO. **(C):** All GFP-positive cells were sorted after a 3-day transduction. Characterization of the sorted cells is shown. Most of the GFP-positive cells are confined to the lymphocyte gate.

confined to the lymphocyte gate (Fig. 2C). These cells were used for repopulation experiments.

Attempts to use cells cultured with FGF-1 for longer than 3 weeks and to shorten or prolong the transduction period resulted in reduction of the percentage of GFP-positive cells (data not shown).

Competitive reconstitution experiments

In order to compare the absolute numbers of HSCs in fresh BM before culture, in the population after culture but before transduction, and in the retrovirus-transduced cell population, we performed limiting dilution and competitive repopulation experiments. Serially reduced numbers of cells from the three sources were transplanted into lethally irradiated recipients, together with 2×10^5 competitor BM cells. At 4, 8, and 10 weeks posttransplant, peripheral blood cells were analyzed to examine the level of donor-derived test cells. The CRU frequencies in unfractionated fresh BM cells, FGF-1-cultured cells, and cultured and then sorted retrovirus-transduced cells were 1/82,000 (with 95% confidence interval 1/34,765–193,475), 1/2700 (1/1399–5211) and 1/3600 (1/1840–7021), respectively (Fig. 3B). Because the starting cell numbers per donor mouse were about 5×10^7 fresh BM cells, $2.5 \pm 0.41 \times 10^7$ FGF-1-cultured cells, and $1.5 \pm 0.41 \times 10^7$ cultured and sorted retrovirus-transduced cells, the absolute numbers of CRUs in each population were calculated to be about 600, 9300 and 4200, respectively. Ultimately, we can conclude that the markedly higher number of retrovirus-transduced HSCs is available in the FGF-1-expanded population

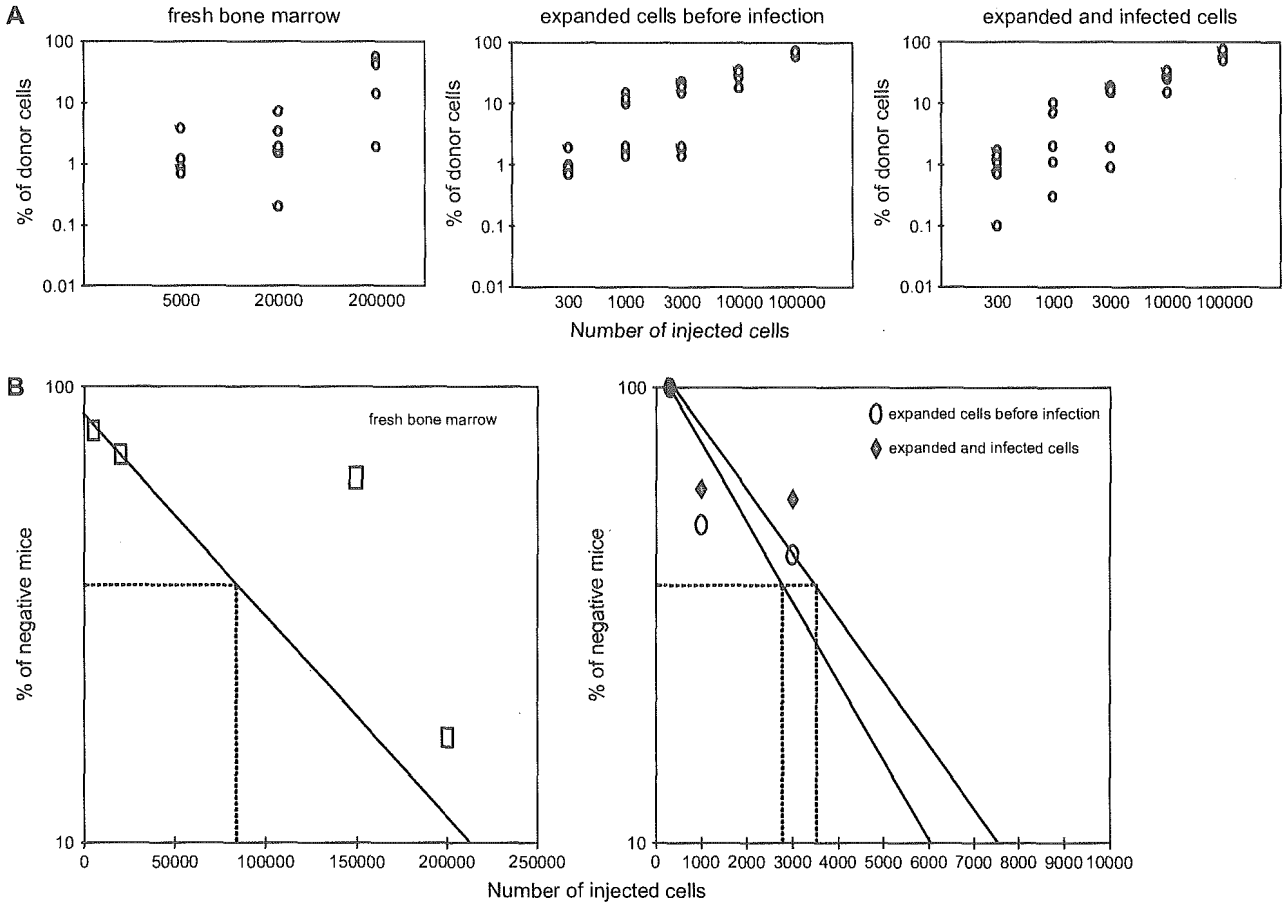

Figure 3. **(A)** Competitive repopulating unit measurements in fresh, FGF-1-expanded and FGF-1-expanded and transduced BM cells. The percentage of donor-derived cells in each cohort of mice is presented. A mouse was considered to be positive if >2% of test cells were detected in both myeloid and lymphoid lineages in the peripheral blood of the recipients 10 weeks after transplant. **(B):** Relation between the test cell dose and the number of engrafted mice was analyzed by Poisson statistics and the CRU frequency is presented.

compared to those in the fresh BM, which should be only a fraction of 600 per mouse.

Contribution of the GFP-positive cells in the recipient mice

To characterize the FGF-1-expanded and retrovirus-transduced HSCs, we transplanted 1×10^5 GFP-positive cells per recipient without competitors. Based on the competitive repopulation assay, this number of retrovirus-transduced cells was expected to provide long-term engraftment. Because the average number of GFP-positive cells that was sorted was about 1.5×10^7 (per experiment initiated from BM cells derived from a single donor mouse), BM cells from a single mouse could be engrafted to 150 recipient mice (Table 1). In the recipient mice, contribution of GFP-positive cells in the myeloid cells was 79 ± 6% at 4 weeks posttransplant. The chimerism was slightly reduced to 67 ± 4.4% but sustained at these levels for 12 weeks. The chimerism of GFP-positive cells in the lymphoid compartment was 43 ± 5% at 4 weeks and slowly increased to 50 ± 6.3% until 12 weeks posttransplant (Fig. 4A and Table 1). We performed transplantation into five to eight recipient mice each in six independent experiments (more than 50 in total), with very consistent results.

Typically, HSCs used for gene delivery are fresh BM cells obtained from 5-FU-treated mice or fresh lineage-negative cells prepared from BM of untreated mice [12–16]. In order to directly compare our protocol with other methods, we transduced freshly purified KSL cells from normal mice with the retrovirus that was used in the transduction of FGF-1-cultured cells. In the transduction procedure, we used a cytokine combination of SCF, TPO, and Flt3 ligand because we had previously evaluated that this combination gave the best results in retrovirus-transduced cell transplantations. After sorting, we transplanted 1×10^3 GFP-positive cells into irradiated recipients. This procedure conferred respective peripheral blood chimerism of 15 ± 5.2% and 7.2 ± 6.1% in the myeloid and lymphoid lineages at 4 weeks posttransplant. However, the chimerism at 12 weeks posttransplant was always

Table 1. Comparison between freshly obtained KSL cells and FGF-1-treated bone marrow as a target for retrovirus-mediated gene delivery

Source	Fresh KSL cells	FGF-1-treated bone marrow
Number of donor mice	10–12	1
Number of available cells before transduction	$5.0 \pm 3.4 \times 10^4$	$2.5 \pm 0.41 \times 10^7$
Number of cells after transduction	$5.0 \pm 2.1 \times 10^4$	$5.2 \pm 0.52 \times 10^7$
Percentage of GFP-positive cells (%)	51 ± 4.1	57 ± 7.7
Number of cells after sorting	$6 \pm 1.2 \times 10^3$	$1.5 \pm 0.41 \times 10^7$
Number of cells injected into one recipient to achieve short-term chimerism w/o competitors	1×10^3	1×10^5
Percentage of donor chimerism at 12 weeks posttransplant		
Myeloid (%)	0.8 ± 0.6	67 ± 4.4
Lymphoid (%)	1.2 ± 1.5	50 ± 6.3
Number of recipient mice	~6	~150

The data is calculated as mean value ± SD from six independent experiments (13 animals for KSL cells and 46 animals for FGF-1-treated bone marrow cells). A parallel comparison of the two sources is given. When using KSL cells the number of mice required to collect only 5×10^4 cells was 10 to 12. This is in contrast to the FGF-1-treated bone marrow cells when just one mouse was used. Still, the number of recipient mice was ~6 and ~150, when using KSL or FGF-1-treated cells, respectively. Furthermore, the later ones provided higher number of GFP-positive cells and higher donor chimerism in the peripheral blood of the recipients 12 weeks after transplant than the previous. KSL, $Lin^-c\text{-}Kit^+Scal^+$ cells; FGF-1, fibroblast growth factor-1; GFP, green fluorescence protein.

<2% in both lineages. The comparison between the FGF-1-cultured cells and freshly obtained KSL cells is summarized in Fig. 4A and Table 1.

The multilineage reconstitution in the peripheral blood of the mice injected with FGF-1-expanded and transduced cells is presented in Figure 4B. Figure 4C demonstrates the contribution of these cells in hematopoietic organs in one of the best reconstituted primary recipients 12 weeks after transplant. On average, chimerism of GFP-positive cells was 41 to 83% in BM, 34 to 75.5% in spleen, 32 to 96.2% in thymus, 15 to 37.1% in lymph nodes, and 31 to 63% in the peritoneal cavity.

Reconstitution of GFP-positive cells in secondary recipients

To further confirm that the retrovirus was integrated in expanded long-term reconstituting cells after the FGF-1 culture, we performed secondary transplantation. Because the mice transplanted with retrovirus-transduced KSL cells showed very low engraftment levels 12 weeks after the primary transplantation, they were not subjected to secondary transplantation. Mice that had received FGF-1-expanded and retrovirus-transduced cells were sacrificed and GFP-positive cells from the BM were sorted. Again, 1×10^5 GFP-positive cells were injected into lethally irradiated secondary recipients (B6-Ly5.2 mice). All mice survived the transplantation. Unlike the primary transplantation in which cultured cells were injected, levels of chimerism in secondary recipients in the peripheral blood were lower at 4 weeks posttransplant in all lineages, but they reached values of 56 ± 7.3% in myeloid and 49 ± 7.6% in lymphoid lineages 8 weeks posttransplant. These levels were maintained at 12 weeks after the secondary transplantation (Fig. 5A). Multilineage reconstitution in the peripheral blood, BM, thymus, spleen, and lymph nodes by GFP-positive cells at 12 weeks after the secondary transplantation in a representative mouse is shown in Figure 5B and C. On average, the percentage of GFP-positive cells was 41 to 85% in BM, 32 to 63% in spleen, 24 to 75% in thymus, 12 to 33% in lymph nodes, and 40 to 63% in the peritoneal cavity. Representative multilineage reconstitution in different organs in a single mouse 12 weeks after the secondary transplantation is presented in Figure 6.

These results indicate that the FGF-1-expanded and subsequently retrovirus-transduced BM cells maintain full multilineage differentiation potential after the serial transplantation in vivo.

It appears that GFP expression levels slightly declined in secondary recipients (Figs. 4C and 5C). This suggests a decrease in the copy number of transgene or partial silencing of vector expression by methylation in serially transplanted HSCs.

Discussion

In this study, we present a method for highly efficient retrovirus transduction into mouse long-term reconstituting cells precultured for 3 weeks in vitro. This is a major challenge to the paradigm that freshly obtained HSCs are the best target for retrovirus-mediated gene transfer because of their presumed highest stem cell potential.

To enrich HSCs and to have them enter the cell cycle are the two major requisites for successful retroviral transduction. To these ends, in mouse HSC transduction, treatment of donor mice with 5-FU and/or antibody- or fluorescent dye-based cell sorting and cytokine treatment during the transduction period have been the most widely used methods in general protocols. In these methods, HSC division necessary for retrovirus transduction depends on selected combinations of exogenous cytokines during a short transduction period as well as in vivo HSC recovery (in the 5-FU strategy).

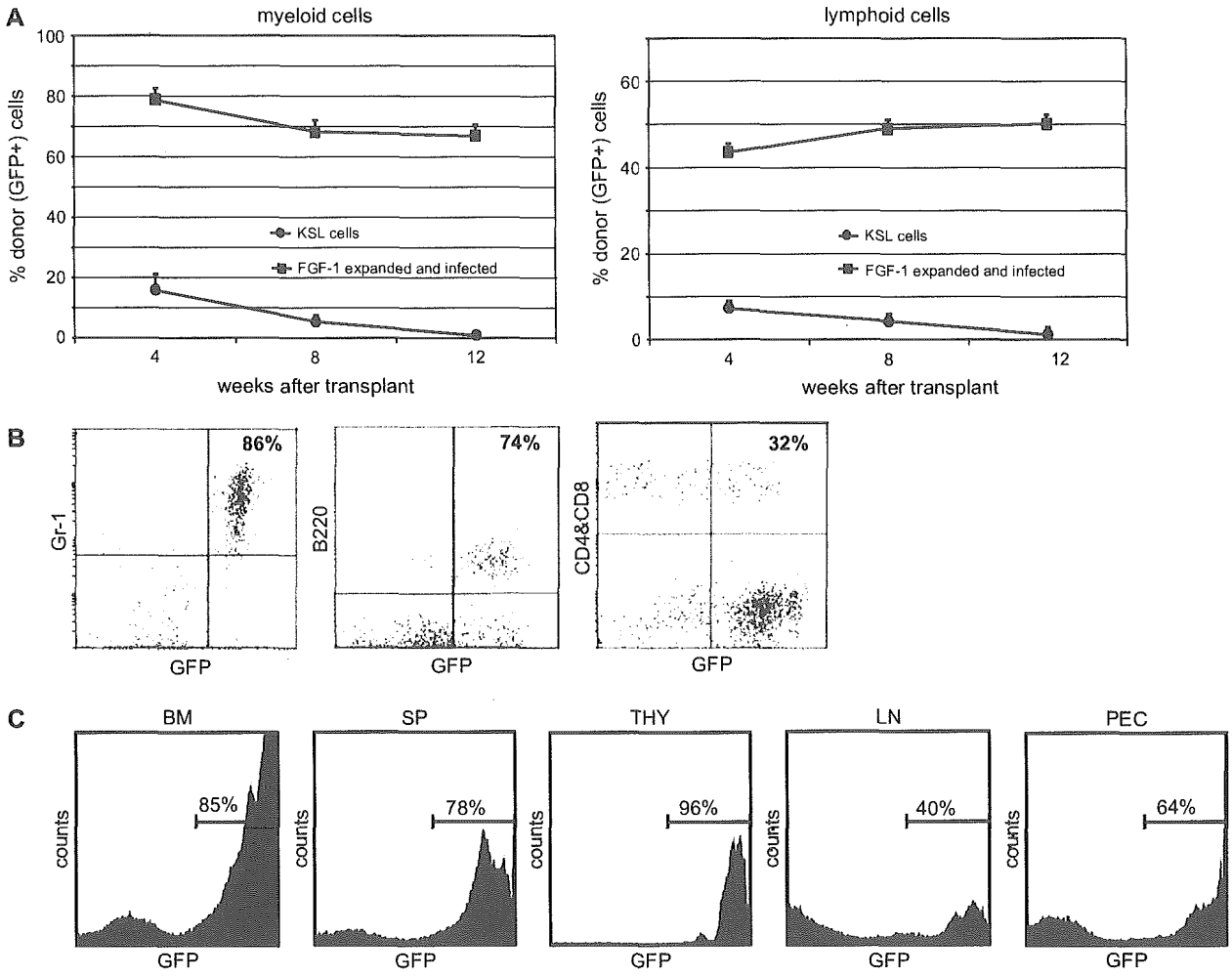

Figure 4. Contribution of GFP-positive cells in the recipient mice 12 weeks after primary transplantation. **(A):** A total of 1×10^5 GFP-positive cells derived from the FGF-1-expanded and retrovirus-transduced culture were transplanted into one group of lethally irradiated recipient mice. In parallel, 1000 GFP-positive KSL cells were transplanted into another group of mice (three to four mice per group were used and the experiment was repeated five times). Engraftment of donor-derived myeloid and lymphoid cells in the recipients at indicated time points after the transplantation is shown. Representative results are shown as the mean ± SD of 46 animals. **(B):** Multilineage reconstitution with GFP-positive cells from the FGF-1-expanded and transduced cells at 12 weeks posttransplant in a representative recipient. **(C):** Contribution of GFP-positive (FGF-1-expanded and transduced) cells in hematopoietic organs of a representative recipient. BM, bone marrow; SP, spleen; THY, thymus; LN, lymph node; PEC, peritoneal cavity.

The lineage-negative population is one of the most frequently used long-term reconstituting cell sources in the study of stem cell biology. However, as a target for retrovirus-mediated gene delivery to HSCs, the KSL population obtained from untreated mice was worse than the FGF-1-expanded population, as shown in Figure 4 and Table 1. The retrovirus transduction efficiency for KSL cells in our experiments appears to be rather lower than those reported by others. This could be biased by sorting of the GFP-positive cells prior to transplantation. Another possibility is that the KSL cells are more difficult to efficiently transduce with retrovirus in comparison to Lin^- or Lin^-Sca1^+ cells maintaining the long-term engraftment potential, as we previously showed [12].

Whole BM cells prepared from 5-FU-treated mice could also be evaluated. Based on our experience and on the literature, the average number of cells available from a single donor mouse is approximately 3×10^6, the transduction efficiency is 40 to 60%, and the CRU frequency is known to be 1/2000 [17,18]. Thus, the absolute number of CRUs that could harbor the retrovirus is estimated to be 600 to 900 per mouse. Comparing these numbers with the results of the limiting dilution study presented in this paper (i.e., actual recovery of 4200 virus-transduced CRUs per mouse), we show that the FGF-1-cultured cells for 3 weeks are a significantly better source of HSCs as a target of retrovirus transduction.

There is an additional advantage in FGF-1-cultured population as a target of gene delivery. Besides the quite high

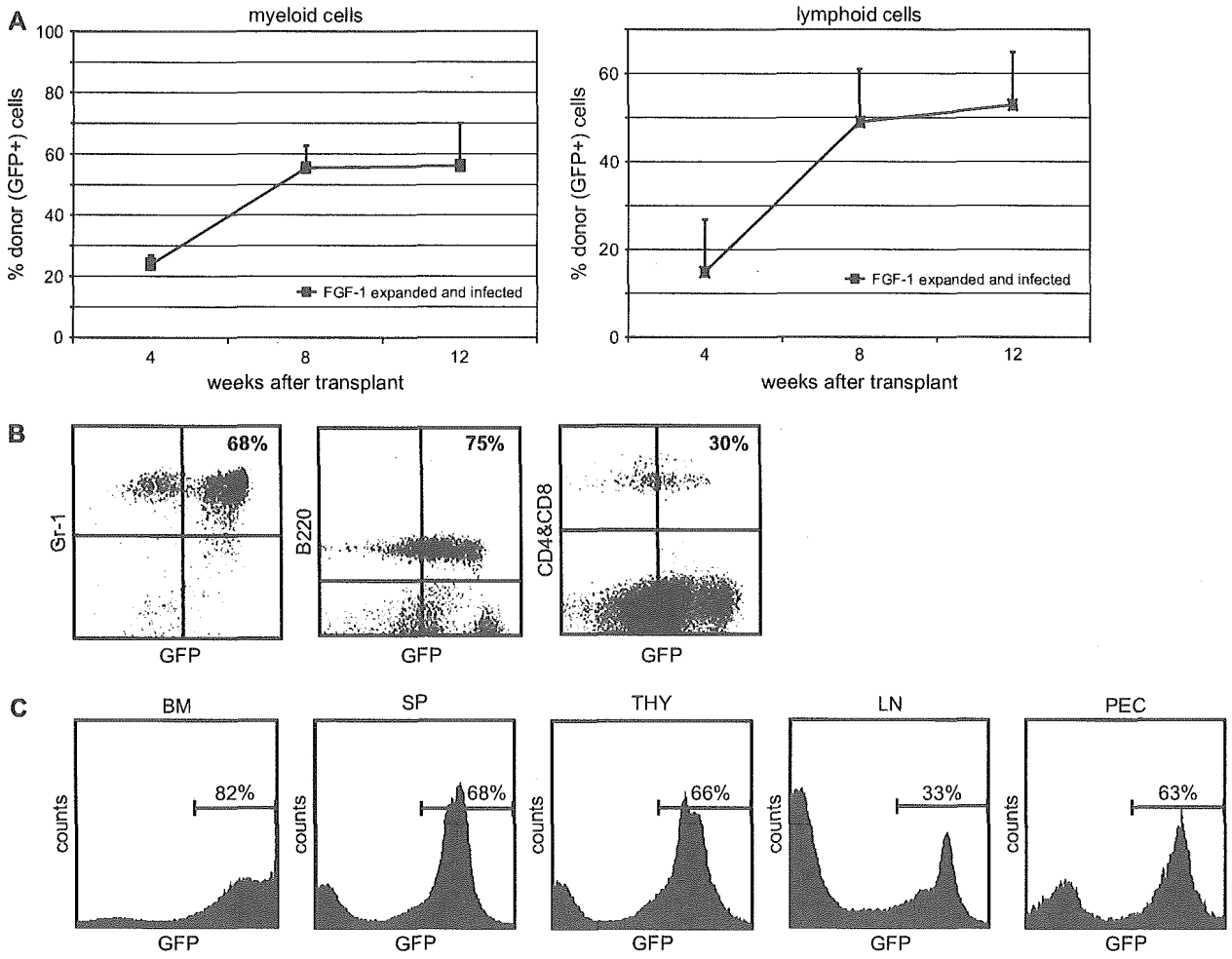

Figure 5. Reconstitution of GFP-positive cells in secondary recipients. A total of 1×10^5 GFP-positive cells were transplanted into lethally irradiated secondary recipients. Chimerism of the donor cells was checked in the peripheral blood of the recipient mice. Engraftment of donor-derived myeloid and lymphoid cells in the transplanted recipients at indicated time points after the transplantation is shown. Representative results are shown as the mean ± SD of 21 animals. **(B):** Multilineage reconstitution in the peripheral blood of a recipient mouse transplanted with GFP-positive cells. **(C):** Contribution of GFP-positive cells in hematopoietic organs of a representative secondary recipient. BM, bone marrow; SP, spleen; THY, thymus; LN, lymph node; PEC, peritoneal cavity.

long-term chimerism, we showed radiation protection and high short-term chimerism with 1×10^5 precultured retrovirus-transduced cells without any rescue cells. This is most likely due to the high ratio of progenitor cells in the FGF-1-expanded and retrovirus-transduced population. The higher short-term chimerism in primary recipients than in secondary ones offers additional support to this conclusion. This is particularly advantageous in experiments in which high chimerism from gene-delivered donor cells is needed. For example, to observe the rescue of the hematolymphopoietic phenotype in the gene knockout mice, this system confers an ideal source of cells for a number of experiments. Indeed, we could rescue a knockout phenotype in the hematopoietic compartment using the protocol described here (data not shown).

It is not completely elucidated in this article whether the quality of FGF-1-expanded HSCs is the same as that of freshly obtained HSCs from BM. In fact, we analyzed the primary recipients 10 weeks after transplant, which could be too short to assess whether the transplanted cells represented true long-term repopulating cells, according to the previous retroviral marking studies. However, we showed long-term and multilineage engraftment at fairly high chimerism levels not only in the primary but also in the secondary recipients. More extensive explorations may reveal similarities and differences between fresh and FGF-1-expanded HSCs.

The robust retroviral transduction of HSCs most probably stems from the expansion of HSCs during the preculture with FGF-1 before transduction. From this consideration, other HSC expansion methods could be chosen for retrovirus transduction protocols, such as the ones using Wnt3a [19,20], Notch ligands [21], and HoxB4 [22]. Compared to these, however, in which HSC purification was required,

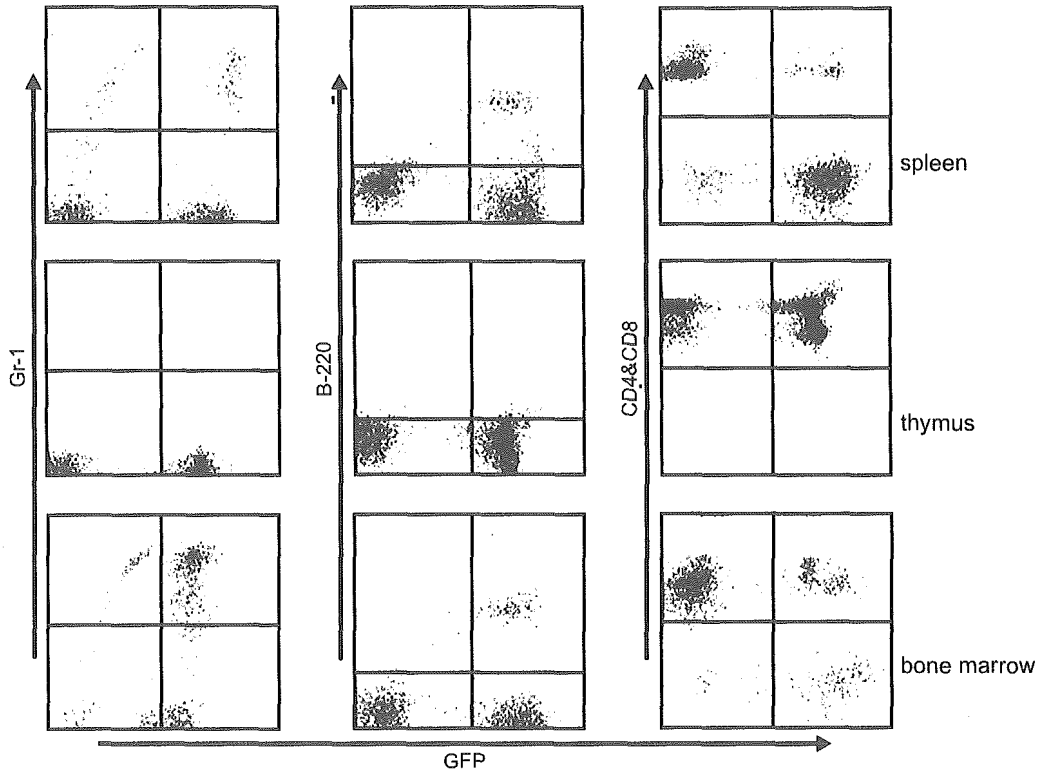

Figure 6. Multilineage reconstitution in secondary recipients. Multilineage reconstitution in the recipient mice was evaluated 12 weeks after the secondary transplantation. Reconstitution in different hematopoietic organs in a representative mouse is shown. bm, bone marrow; sp, spleen; thy, thymus. The cells from different organs were stained with Gr1 (for myeloid cells), B220 (for B cells), and CD4 and CD8 (for T cells). Engraftment of donor-derived granulocytes, B cells, and T cells is shown.

the method utilized here is unique in that we use whole BM cells without any purification, serving a very simple protocol. Moreover, FGF-1 is available on the market unlike Wnt3a or Notch ligands. Owing to this, it was easy to examine the reproducibility of HSC expansion by ourselves.

In our current experiments, MOI was calculated to be in the range between 300–340 and 1.1 to 1.2 $\times$ 10^4 for FGF-1-expanded and KSL cells, respectively. These values could be too high and may have yielded high transgene copy numbers [23]. It would be desirable to test the retroviral copy numbers; if they are high, we need to improve our gene transfer protocol.

The increase in the number of cells during the 3-day transduction period is possibly due to the preculture with FGF-1 together with heparin and to the combination of SCF, TPO, and FGF-1 without heparin during the transduction period. During this period, FGF-1 alone did not support cell growth nor virus transduction (Fig. 2A), and addition of other mitogenic cytokines such as the combination of SCF + TPO was required. This is probably due to the removal of the heparin, which is required to maximize the biologic activity of FGF-1, but on the other hand, its addition lowers the transduction efficiency [24].

Regarding the cytokines to be used during the transduction procedure, there is still no general agreement, and the use of a SCF + TPO combination was based on experience. Different research groups have reported diverse combinations [14,25]. The synergy between SCF and TPO has been reported [26–29], and our group has previously shown that this combination works well for retroviral transduction [11,30]. In the current protocol, FGF-1 was further added to that cytokine combination because it preserved the amount of KS cells slightly better than the combination without FGF-1 (Fig. 2B).

We did not examine whether the retrovirus-transduced HSCs were further expandable ex vivo, either in the presence of FGF-1 or supernatant in which the cells were grown. This is an interesting issue to be answered, particularly if the expansion efficiency is improved.

Consequently, the protocol introduced here using a retroviral vector for HSC gene transduction can be as efficient as protocols utilizing lentiviral vectors and superior to those with respect to the number of gene-transduced HSCs.

In conclusion, whole BM cells cultured in the presence of FGF-1 for 3 weeks provide HSCs highly competent to retrovirus transduction and can be of great value for the retrovirus-transduced HSC transplantation experiments.

Acknowledgments

A.C. is supported by a fellowship from the Ministry of Education, Culture, Sports, Science and Technology of Japan. This study was supported by Special Coordination Funds for Promoting Science and Technology from the Ministry of Education, Culture, Sports, Science and Technology of Japan, and Research on Pharmaceutical and Medical Safety, Health and Labor Sciences Research Grants from the Ministry of Health, Labor and Welfare of Japan. We express our deepest gratitude to Hisamaru Hirai, deceased in August, 2003. We also thank Toshio Suda and Fumio Arai of Keio University for their valuable discussions.

References

1. Conneally E, Cashman J, Petzer A, Eaves C. Expansion in vitro of transplantable human cord blood stem cells demonstrated using a quantitative assay of their lympho-myeloid repopulating activity in nonobese diabetic-scid/scid mice. Proc Natl Acad Sci U S A. 1997; 94:9836–9841.
2. Miller CL, Eaves CJ. Expansion in vitro of adult murine hematopoietic stem cells with transplantable lympho-myeloid reconstituting ability. Proc Natl Acad Sci U S A. 1997;94:13648–13653.
3. Zandstra PW, Conneally E, Petzer AL, Piret JM, Eaves CJ. Cytokine manipulation of primitive human hematopoietic cell self-renewal. Proc Natl Acad Sci U S A. 1997;94:4698–4703.
4. Bodine DM, McDonagh KT, Seidel NE, Nienhuis AW. Survival and retrovirus infection of murine hematopoietic stem cells in vitro: effects of 5-FU and method of infection. Exp Hematol. 1991;19:206–212.
5. Stewart FM, Crittenden RB, Lowry PA, Pearson-White S, Quesenberry PJ. Long-term engraftment of normal and post-5-fluorouracil murine marrow into normal nonmyeloablated mice. Blood. 1993;81:2566–2571.
6. de Haan G, Weersing E, Dontje B, et al. In vitro generation of long-term repopulating hematopoietic stem cells by fibroblast growth factor-1. Dev Cell. 2003;4:241–251.
7. Misawa K, Nosaka T, Morita S, et al. A method to identify cDNAs based on localization of green fluorescent protein fusion products. Proc Natl Acad Sci U S A. 2000;97:3062–3066.
8. Yoshimatsu T, Tamura M, Kuriyama S, Ikenaka K. Improvement of retroviral packaging cell lines by introducing the polyomavirus early region. Hum Gene Ther. 1998;9:161–172.
9. Miller AD, Buttimore C. Redesign of retrovirus packaging cell lines to avoid recombination leading to helper virus production. Mol Cell Biol. 1986;8:2895–2902.
10. Mann R, Mulligan RC, Baltimore D. Construction of a retrovirus packaging mutant and its use to produce helper-free defective retrovirus. Cell. 1983;1:153–159.
11. Osawa M, Hanada K, Hamada H, Nakauchi H. Long-term lymphohematopoietic reconstitution by a single 34-low/negative hematopoietic stem cell. Science. 1996;273:242–245.
12. Kunisato A, Chiba S, Nakagami-Yamaguchi E, et al. HES-1 preserves purified hematopoietic stem cells ex vivo and accumulates side population cells in vivo. Blood. 2003;101:1777–1783.
13. Lemischka IR, Raulet DH, Mulligan RC. Developmental potential and dynamic behavior of hematopoietic stem cells. Cell. 1986;45:917–927.
14. Pear WS, Miller JP, Xu L, et al. Efficient and rapid induction of a chronic myelogenous leukemia-like myeloproliferative disease in mice receiving P210 bcr/abl-transduced bone marrow. Blood. 1998; 92:3780–3792.
15. Antonchuk J, Sauvageau G, Humphries RK. HOXB4-induced expansion of adult hematopoietic stem cells ex vivo. Cell. 2002;109:39–45.
16. Varnum-Finney B, Xu L, Brashem-Stein C, et al. Pluripotent, cytokine-dependent, hematopoietic stem cells are immortalized by constitutive Notch1 signaling. Nat Med. 2000;6:1278–1281.
17. Szilvassy SJ, Humphries RK, Lansdorp PM, Eaves AC, Eaves CJ. Quantitative assay for totipotent reconstituting hematopoietic stem cells by a competitive repopulation strategy. Proc Natl Acad Sci U S A. 1990;87:8736–8740.
18. Szilvassy SJ, Lansdorp PM, Humphries RK, Eaves AC, Eaves CJ. Isolation in a single step of a highly enriched murine hematopoietic stem cell population with competitive long-term repopulating ability. Blood. 1989;74:930–939.
19. Reya T, Duncan AW, Ailles L, et al. A role for Wnt signalling in self-renewal of haematopoietic stem cells. Nature. 2003;423:409–414.
20. Willert K, Brown JD, Danenberg E, et al. Wnt proteins are lipid-modified and can act as stem cell growth factors. Nature. 2003;423:448–452.
21. Calvi LM, Adams GB, Weibrecht KW, et al. Osteoblastic cells regulate the haematopoietic stem cell niche. Nature. 2003;425:841–846.
22. Krosl J, Austin P, Beslu N, et al. In vitro expansion of hematopoietic stem cells by recombinant TAT-HOXB4 protein. Nat Med. 2003;11: 1428–1432.
23. Li Z, Schwieger M, Lange C, et al. Predictable and efficient retroviral gene transfer into murine bone marrow repopulating cells using a defined vector dose. Exp Hematol. 2003;31:1206–1214.
24. Carstanjen D, Dutt P, Moritz T. Heparin inhibits retrovirus binding to fibronectin as well as retrovirus gene transfer on fibronectin fragments. J Virol. 2001;75:6218–6222.
25. Srour EF, Abonour R, Cornetta K, Traycoff CM. Ex vivo expansion of hematopoietic stem and progenitor cells: are we there yet? J Hematother. 1999;8:93–102.
26. Sitnicka E, Lin N, Priestley GV, et al. The effect of thrombopoietin on the proliferation and differentiation of murine hematopoietic stem cells. Blood. 1996;87:4998–5005.
27. Ku H, Yonemura Y, Kaushansky K, Ogawa M. Thrombopoietin, the ligand for the Mpl receptor, synergizes with steel factor and other early acting cytokines in supporting proliferation of primitive hematopoietic progenitors of mice. Blood. 1996;87:4544–4551.
28. Ramsfjell V, Borge OJ, Veiby OP, et al. Thrombopoietin, but not erythropoietin, directly stimulates multilineage growth of primitive murine bone marrow progenitor cells in synergy with early acting cytokines: distinct interactions with the ligands for c-kit and FLT3. Blood. 1996; 88:4481–4492.
29. Ema H, Takano H, Sudo K, Nakauchi H. In vitro self-renewal division of hematopoietic stem cells. J Exp Med. 2000;192:1281–1288.
30. Kunisato A, Chiba S, Saito T, et al. Stem cell leukemia protein directs hematopoietic stem cell fate. Blood. 2004;103:3336–3341.

Host-Residual Invariant NK T Cells Attenuate Graft-versus-Host Immunity[1]

Kyoko Haraguchi,*† Tsuyoshi Takahashi,*[2] Akihiko Matsumoto,*† Takashi Asai,* Yoshinobu Kanda,*† Mineo Kurokawa,* Seishi Ogawa,*‡ Hideaki Oda,§ Masaru Taniguchi,¶ Hisamaru Hirai,[3]*† and Shigeru Chiba[4]*†

Invariant NK T (iNKT) cells have an invariant TCR-α chain and are activated in a CD1d-restricted manner. They are thought to regulate immune responses and play important roles in autoimmunity, allergy, infection, and tumor immunity. They also appear to influence immunity after hemopoietic stem cell transplantation. In this study, we examined the role of iNKT cells in graft-vs-host disease (GVHD) and graft rejection in a mouse model of MHC-mismatched bone marrow transplantation, using materials including α-galactosylceramide, NKT cells expanded in vitro, and Jα18 knockout mice that lack iNKT cells. We found that host-residual iNKT cells constitute effector cells which play a crucial role in reducing the severity of GVHD, and that this reduction is associated with a delayed increase in serum Th2 cytokine levels. Interestingly, we also found that host-residual iNKT cause a delay in engraftment and, under certain conditions, graft rejection. These results indicate that host-residual iNKT cells attenuate graft-vs-host immunity rather than host-vs-graft immunity. *The Journal of Immunology,* **2005, 175: 1320–1328.**

Natural killer T cells are a population of T cells that have NK cell markers such as NK1.1 (NKR-P1C) in mice or CD161 (NKR-P1A) in humans (1, 2). Some NK T cells use an invariant TCR-α chain (Vα14-Jα18 in mice, Vα24-Jα18 in humans) paired with Vβ8, Vβ7, or Vβ2 in mice or with Vβ11 in humans (3–7), and are called invariant NKT (iNKT)[5] cells. iNKT cells are activated by synthetic glycolipids such as α-galactosylceramide (α-GalCer) in a CD1d-restricted manner (1, 2, 8, 9). iNKT cells produce both Th1 (such as IFN-γ and TNF-α) and Th2 (such as IL-4, IL-5, IL-10, and IL-13) cytokines (1, 2, 8, 9). It has been reported that iNKT cells control immune responses in some infections, tumors, autoimmune diseases, and allograft rejection (1, 2, 8, 9).

Graft-vs-host disease (GVHD) is one of the most serious complications in hemopoietic stem cell transplantation. It has been suggested in a mouse acute GVHD model that NK1.1$^+$ T cells obtained from donor bone marrow can suppress GVHD induced by peripheral blood transplantation from the same donor (10). It has also been shown that a selected conditioning regimen, which preserves more host-residual NK1.1$^+$ or DX5$^+$ T cells than other T cells, is advantageous for reducing acute GVHD (11, 12). Furthermore, the suppressive effect of α-GalCer on induced acute GVHD has been demonstrated in a mouse model(13, 14). We previously reported that the number of iNKT cells was lower in patients with GVHD than in those without GVHD (15) after hemopoietic stem cell transplantation, although the cause-effect relationship was not clear.

In this report, we provide direct evidence that host-residual iNKT cells reduce GVHD in a mouse model of MHC-mismatched bone marrow transplantation using Jα18 knockout mice that lack iNKT cells (16). Adoptively transferred iNKT cells with grafts also reduce GVHD, but, importantly, this effect is dependent on the presence of host-residual iNKT cells.

Materials and Methods

Mice

C57BL/6 (H-2^b) and BALB/c (H-2^d) mice were purchased from Japan Clea. Jα18 knockout mice (16) were kindly provided by M. Harada (Chiba University, Chiba, Japan) and bred in the University of Tokyo animal facility. Drinking water for bone marrow transplant recipients was supplemented with 25 μg/ml neomycin sulfate and 0.3 U/ml polymyxin B (Sigma-Aldrich). Mouse studies were conducted according to the University of Tokyo Animal Experiment Manual.

Abs and reagents

The following Abs were purchased from BD Pharmingen: anti-CD4 (RM4-5), CD8α (53-6.7), CD45R/B220 (RA3-6B2), NK1.1 (PK136), H2D^b (KH95), H2D^d (34-2-12), I-A^b (AF6-120.1), I-A^d (39-10-8), LY-6G (Gr-1)/Ly6C (RB6-8C5), TCRβ(H57-597), and CD16/CD32 (2.4G2). α-GalCer was kindly provided by Kirin Brewery. Rabbit anti-asialo GM1 Ab was purchased from Wako Biochemicals. Murine rIL-7 and IL-15 were purchased from PeproTech. Human rIL-2 was kindly provided by Shionogi. Murine CD1d tetramer was established by Dr. M. Kronenberg (La Jolla Institute for Allergy and Immunology, La Jolla, CA) (17) and kindly provided by Dr. Nakayama (Chiba University, Chiba, Japan).

GVHD model

Six- to 8-week-old BALB/c hosts were given total-body irradiation (8 Gy) from a 150-Kv x-ray source and injected with donor cells via the tail vein within 6 h. All mice received 1 × 10^7 bone marrow cells and 1 × 10^7

Departments of *Hematology/Oncology, †Cell Therapy/Transplantation Medicine, and ‡Regeneration Medicine for Hematopoiesis, University of Tokyo Graduate School of Medicine and Hospital, Tokyo, Japan; §Department of Pathology, Tokyo Women's Medical University, Tokyo, Japan; and ¶RIKEN Research Center for Allergy and Immunology, Yokohama, Japan

Received for publication December 9, 2004. Accepted for publication April 21, 2005.

The costs of publication of this article were defrayed in part by the payment of page charges. This article must therefore be hereby marked *advertisement* in accordance with 18 U.S.C. Section 1734 solely to indicate this fact.

[1] **This work was supported in part by a Grant-in-Aid for Scientific Research,** KAKENHI (14370300), and Research on Regulatory Sciences of Pharmaceuticals and Medical Devices, Health and Labour Sciences Research Grants, Ministry of Health, Labour and Welfare of Japan.

[2] Current address: Division of Immunology & Rheumatology, Stanford University School of Medicine, Palo Alto, CA.

[3] Hisamaru Hirai died on August 23, 2003.

[4] Address correspondence and reprints requests to Dr. Shigeru Chiba, Department of Cell Therapy and Transplantation Medicine, University of Tokyo, 7-3-1 Hongo, Bunkyo-ku, Tokyo 113-8655, Japan. E-mail address: schiba-tky@umin.ac.jp

[5] Abbreviations used in this paper: iNKT, invariant NK T; α-GalCer, α-galactosylceramide; GVHD, graft-vs-host disease; CBA, cytometric bead array, cRPMI, complete RPMI.

0022-1767/05/$02.00

spleen cells obtained from C57BL/6 or BALB/c. Donor mice were 6–10 wk old and the same sex as the hosts. For α-GalCer treatment, mice received 2 μg/mouse (18, 19) α-GalCer, corresponding to ~100 μg/kg (20, 21), or control vehicle i.p. every 4 days from day 0 or −4 of transplantation. For the iNKT adoptive transfer model, mice received 1×10^6 in vitro-expanded iNKT cells with donor cells. For in vivo NK cell depletion, mice received 20 μl of rabbit anti-asialo GM1 Ab on days −5 and −1 or on day −1 of transplantation. We used the same amount of PBS as a control. Survival and appearance were monitored daily and body weight was measured every other day. GVHD was assessed by a scoring system that summed changes in five clinical parameters: weight loss, posture, activity, fur texture, and skin integrity (maximum index = 10) as previously described (22). Histopathological specimens from the skin, liver, and intestine of 15 dying mice were obtained on days 5–59 (median, 18 days) after transplantation and were stained with H&E.

Serum cytokines

Serum was obtained from recipient mice at 3- 6 h (early phase) or on day 5 or 6 posttransplant and stored at −20°C. IL-2, IL-4, IL-5, TNF-α, and IFN-γ were detected simultaneously using the mouse Th1/Th2 cytokine cytometric bead array (CBA) kit (BD Pharmingen).

In vitro stimulation of immunized splenocytes with α-GalCer

BALB/c mice were injected with α-GalCer (2 μg/mouse) or control vehicle i.p. and sacrificed 6 days after the injection. Splenocytes (1×10^5) were incubated with 100 ng/ml α-GalCer or control vehicle in RPMI 1640 medium supplemented with 10% FCS, penicillin-streptomycin, and 50 μM β-ME (complete RPMI (cRPMI)) for 72 h. The supernatants were collected and measured for the concentrations of cytokines using the mouse Th1/Th2 cytokine CBA kit.

Chimerism

We sacrificed mice on days 3–14 (median, 5 days) posttransplant. Splenocytes were stained with H-2D^b-FITC or H-2D^d-FITC, CD4-PE and CD8-allophycocyanin Abs. Bone marrow cells were stained with H-2D^b-FITC or H-2D^d-FITC and Gr-1-PE Abs. To analyze NKT chimerism, hepatic mononuclear cells were prepared as previously described (20) and stained with H-2D^b-FITC or H-2D^d-FITC, α-GalCer-loaded murine CD1d tetramer-PE and TCRβ-allophycocyanin Abs. Propidium iodine (BD Biosciences) was used to exclude dead cells. Immunofluorescence staining was performed according to standard procedures (15). Cells were analyzed by FACSCalibur and CellQuest software (BD Biosciences).

In vitro culture of iNKT cells

Vα14$^+$ NKT cells were established as follows. Thymocytes of 5- to 7-wk-old C57BL/6 and BALB/c mice were pretreated with anti-CD16/CD32 Abs to block FcγR and incubated with NK1.1-PE (C57BL/6) or α-GalCer-loaded CD1d tetramer (BALB/c), followed by anti-PE microbeads, and sorted by positive magnetic bead sorting (MACS; Miltenyi Biotec). Splenic dendritic cells were obtained in a standard procedure. In short, spleens were injected with 100 U/ml collagenase D (Roche Diagnostics) and minced. After the incubation in collagenase D for 45 min at 37°C, the spleen fragments were passed through a steel mesh and RBCs were lysed. The cells were cultured overnight in cRPMI with 30 ng/ml α-GalCer. Nonadherent cells were sorted by CD11c Microbeads (Miltenyi Biotec). NK1.1- or α-GalCer-loaded CD1d tetramer-positive thymocytes were cultured for 7 days with irradiated (15 Gy) α-GalCer-pulsed splenic dendritic cells in cRPMI supplemented with human IL-2 (30 U/ml), murine IL-7 (40 ng/ml), murine IL-15 (50 ng/ml), and α-GalCer (30 ng/ml).

In vitro cytokine production by cultured iNKT cells

For in vitro cytokine production assay, 5×10^4 Vα14$^+$ NKT cells and 5×10^4 α-GalCer-pulsed splenic dendritic cells were suspended in 200 μl of cRPMI and cultured in 96-well plates. After 24 h, the supernatants were collected from each well and assayed for the concentrations of cytokines using the mouse Th1/Th2 cytokine CBA kit.

Molecular analysis of TCR-α transcripts

Total RNA was extracted from 1×10^6 NKT cells according to the manufacturer's protocol (Tri Reagent LS; Sigma-Aldrich) and reverse transcribed. The transcribed cDNA was subjected to PCR amplification using the primer pair (5′-CTAAGCACAGCACGCTGCACA-3′, Vα14; and 5′-TGGCGTTG GTCTCTTTGAAG-3′, Cα) or the pair for β-actin (5′-GAGAGGGA AATCGTGCGTGA-3′ and 5′-ACATCTGCTGGAAGGTGGAC-3′) under the following conditions: 94°C for 60 s, 60°C for 60 s, and 72°C for 60 s for 40 cycles as described previously (7). For detection of the Vα-Jα sequence, the DNA band was excised from the agarose gel and DNA was extracted and purified according to the manufacturer's protocol (QIAquick Gel Extraction kit; Qiagen). Nucleotide sequences were determined by an ABI PRISM 310 Genetic Analyzer (Applied Biosystems). The primer used for sequencing was 5′-TGGCGTTGGTCTCTTTGAAG-3′.

Statistical analysis

Mouse survival was analyzed by the log-rank test. GVHD scores in the two groups were compared using repeated measures ANOVA. Differences in the proportion of iNKT cells and the chimerism were analyzed using Student's *t* test. The cytokine levels in serum were analyzed using the nonparametric Mann-Whitney *U* test. A $p < 0.05$ was considered to be significant.

Results

Establishment of GVHD model mice

In the prototype transplantation from wild-type C57BL/6 to wild-type BALB/c, all of the recipients showed lethal GVHD as judged by the GVHD score. Histological examinations also confirmed GVHD in representative mice (data not shown). In this setting, we confirmed that full donor chimerism was achieved in all of the recipients (data not shown). We performed all of the transplantation experiments two to four times independently, and integrated all of the results from individual experiments to avoid experiment-to-experiment variation.

Administration of α-GalCer prolonged survival of GVHD mice

First, we administered either α-GalCer to activate iNKT cells or control vehicle every 4 days from the day of transplantation. α-GalCer-treated mice survived significantly longer than control mice ($p < 0.0001$, Fig. 1*A*). The severity of GVHD in α-GalCer-treated mice was milder than that in control mice (Fig. 1*B*). The GVHD score within the first 30 days after transplantation in the two groups was compared by repeated measures ANOVA and was found to be significantly lower in the α-GalCer group ($p < 0.0001$).

We then examined whether α-GalCer treatment influenced the number of iNKT cells in the liver, which contains the largest proportion of iNKT cells (1, 9) (14.2 ± 4.7% in our measurements; Fig. 1*Di*), after transplantation. In control recipients, the ratio of iNKT cells to lymphocytes decreased rapidly and iNKT cells became undetectable by approximately day 5 posttransplant (Fig. 1, *C* and *D*). The rate of decrease in the iNKT cells was delayed in α-GalCer-treated mice, although iNKT cells were scarcely detectable after day 10 even in mice treated with α-GalCer (Fig. 1*C*). We observed temporary donor-type iNKT cell chimerism before the disappearance, although the time course of the donor:recipient iNKT cell ratio was highly variable (data not shown).

Interestingly, we found that the engraftment of donor CD4$^+$ T cells in α-GalCer-treated mice was delayed compared with that in control mice during the early phase after transplantation, although complete donor chimerism was eventually achieved (Fig. 2*A*). Engraftment of Gr-1$^+$ cells was also slightly delayed, but engraftment of other lineage cells was similar to that seen in vehicle-treated mice (data not shown). These findings encouraged us to compare various cytokine levels between α-GalCer-treated and control mice, since iNKT cells produce high levels of both Th1 and Th2 cytokines and could influence Th1/Th2 polarization. Therefore, we examined the serum levels of IFN-γ, TNF-α, IL-4, and IL-5 shortly after transplant and found that all of the cytokines were increased by α-GalCer treatment (Fig. 2*B*, *i-iv*), reproducing previous reports that α-GalCer has been shown to rapidly stimulate Th1 and Th2 cytokine production in vivo in the nontransplantation

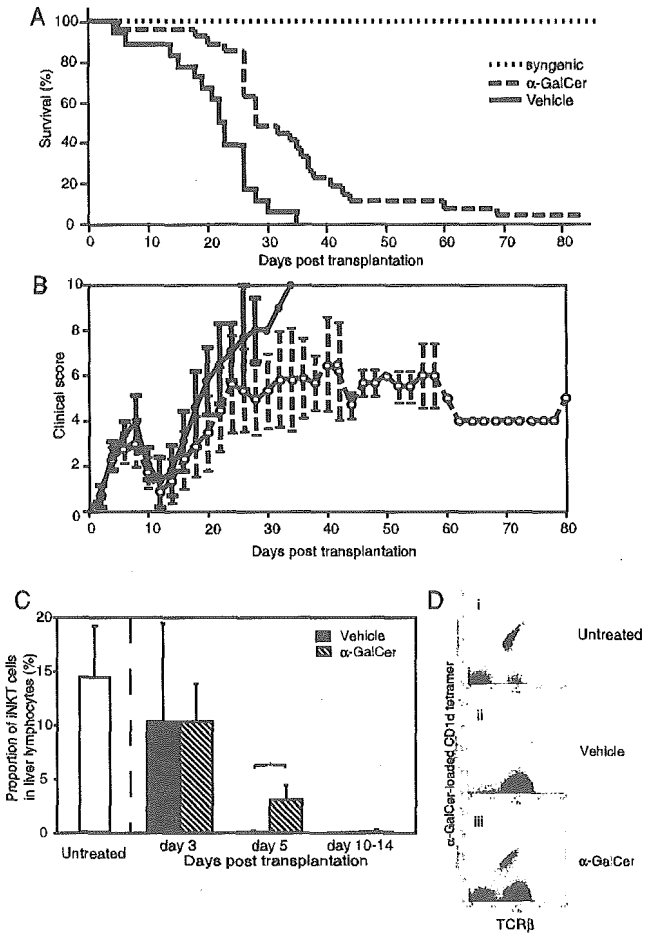

FIGURE 1. Survival of α-GalCer-treated GVHD mice. *A*, Survival of α-GalCer-treated (n = 27) mice, control vehicle-treated (n = 18) GVHD mice, and syngeneic cell-transplanted mice (n = 7). α-GalCer-treated GVHD mice survived longer than vehicle-treated GVHD mice ($p < 0.0001$). *B*, Mean clinical score and SD of α-GalCer-treated and vehicle-treated GVHD mice. The GVHD score was determined from the surviving mice shown in *A*. Within the first 30 days after transplantation, the GVHD score was significantly lower in the α-GalCer-treated group ($p < 0.0001$). *C*, Proportion of iNKT cells in liver lymphocytes from untreated mice and those early after transplantation. We analyzed liver iNKT cells from 6 vehicle- and 6 α-GalCer-treated recipients on day 3, 9 vehicle- and 11 α-GalCer-treated recipients on day 5, and 10 vehicle- and 10 α-GalCer-treated recipients on days 10–14 (median, 11 days). There is a statistically significant difference between the proportions of liver iNKT cells from vehicle- and α-GalCer-treated recipients on day 5 posttransplant ($p < 0.0001$). *D*, Representative FACS dot plots for liver iNKT cells from mice on day 5 posttransplant or an untreated mouse.

model (23–25). In contrast, it has been reported that in vivo α-GalCer-primed splenocytes secrete less amounts of Th1 cytokines after further in vitro treatment with α-GalCer compared with vehicle-primed splenocytes (23, 26). In our experimental system, we could exactly reproduce these findings (Fig. 2*C*, *i-iv*). Then we measured all four cytokines on day 5 or 6 posttransplant (1 or 2 days after the second α-GalCer administration), both in α-GalCer- and vehicle-treated mice. At this time point, GVHD signs were not been obvious yet, although the damage from radiation was inseparably measured "GVHD score" in Fig. 1*B*. IFN-γ and TNF-α levels in α-GalCer-treated mice were significantly lower than those in control mice, whereas levels of IL-4 and IL-5 in α-GalCer-treated mice were significantly higher in α-GalCer-treated mice (Fig. 2*D*, *i-iv*). These findings suggested that the administration of repeated α-GalCer somehow influenced cytokine production by iNKT cells, which resulted in a difference in the engraftment of donor $CD4^+$ T cells and a shift to the Th2 cytokine pattern early after transplantation.

iNKT adoptive transfer prolonged survival of GVHD mice

To obtain more direct evidence that the regulatory function of α-GalCer is mediated through iNKT cells, we first examined whether adoptively transferred iNKT cells attenuate GVHD. NK1.1- or α-GalCer-loaded CD1d tetramer-positive thymocytes from either C57BL/6 or BALB/c mice, respectively, were enriched and expanded in vitro. The purity of α-GalCer-loaded CD1d tetramer-positive cells after expansion was 90–98% (median, 95%) (Fig. 3*A*). To confirm that most of the in vitro-expanded NKT cells use the invariant TCR α-chain, we performed RT-PCR on RNA from the cells using the Vα14 and Cα primers and analyzed a fragment encompassing the V-J junction. The sequence of the RT-PCR product (Fig. 3*B*) was GCCACCTACATCTGGTGGT GGGCGATAGAGGTTCAGCCTTAGGGAGGCTGCATTTT, which is compatible with the sequence of the Vα14-Jα18 invariant chain. Furthermore, we checked in vitro function of expanded iNKT cells. Stimulation by autologous (or allogeneic, data not shown) dendritic cells in the presence of α-GalCer induced iNKT cells to produce a higher amount of cytokines compared with that in the presence of vehicle. This cytokine production was blocked by anti-CD1d Ab (Fig. 3*C*, *i-iv*).

These iNKT cells (1×10^6) were transferred along with the C57BL/6-derived graft (2×10^7) to irradiated BALB/c mice. As a control, the same amount (2×10^7) of C57BL/6-derived graft alone was used. The 5% difference in the total cell number was within the range of error. These recipient mice survived significantly longer than control mice, regardless of whether the adoptively transferred iNKT cells were derived from C57BL/6 or BALB/c mice ($p < 0.001$ Fig. 3*D*). To see whether transferred iNKT cells had expanded in the recipients, we examined iNKT cells in the liver lymphocytes. On days 5–7 posttransplant, there were very few iNKT cells in the liver of control mice that received grafts without adoptive iNKT cells (Fig. 3*Ei*). In contrast, iNKT cells were clearly detected on the same days in the liver of recipient mice that had been transplanted with grafts containing adoptive iNKT cells. This observation was independent of whether the transferred iNKT cells were derived from C57BL/6 or BALB/c mice (Fig. 3*E*, *ii-iii*). Surprisingly, if the origin of the adopted iNKT cells was the same as the donor strain (C57BL/6), both H-$2D^d$-negative (C57BL/6-derived) and H-$2D^d$-positive (BALB/c-derived) iNKT cells were reproducibly detected (Fig. 3*Ev*). Similarly, if the origin of the adopted iNKT cells was the same as the host strain (BALB/c), both BALB/c-derived and C57BL/6-derived iNKT cells were reproducibly detected (Fig. 3*Eiv*). The former result indicates that the adopted donor strain iNKT cells were temporarily engrafted and helped host-residual iNKT cells remain. The latter result indicates that the adopted host strain iNKT cells were engrafted or helped host-residual iNKT cells remain and further helped graft-contaminated iNKT cells be engrafted temporarily.

Then we measured serum cytokines shortly after transplantation with adoptive iNKT transfer. The serum cytokine levels in the iNKT-transferred mice were higher than those in the recipient mice without iNKT cell transfer. Therefore, iNKT cell transfer mimics the α-GalCer administration in the acute phase cytokine production profile in the recipient mice.

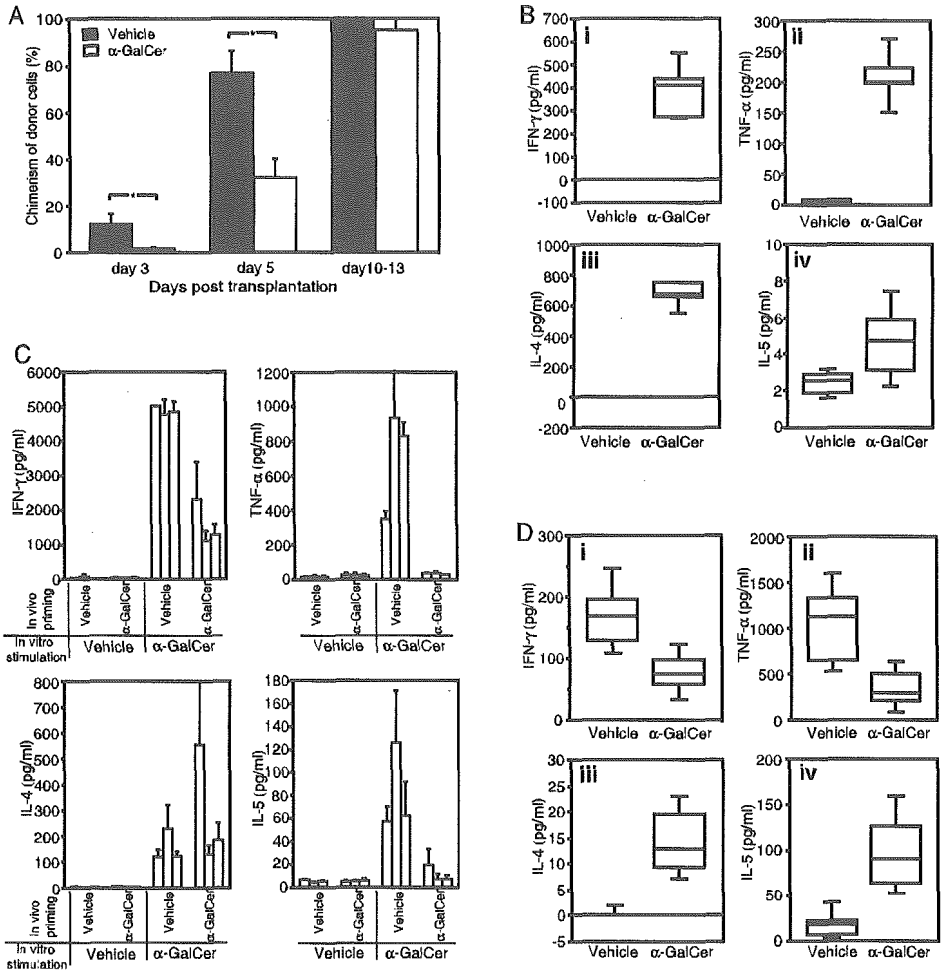

FIGURE 2. $CD4^+$ splenocyte chimerism and serum cytokines of α-GalCer-treated mice. *A*, Chimerism of $CD4^+$ splenocytes in α-GalCer and vehicle-treated recipients. We analyzed $CD4^+$ splenocytes from 6 vehicle- and 6 α-GalCer-treated recipients on day 3, 9 vehicle- and 11 α-GalCer-treated recipients on day 5, and 8 vehicle- and 8 α-GalCer-treated recipients on days 10–13 (median, 11 days). There is a statistically significant difference between the proportions of $CD4^+$ splenocytes from vehicle- and α-GalCer-treated recipients on day 3 ($p = 0.002$) and day 5 ($p < 0.0001$) posttransplant ($p < 0.0001$). *B*, Composite box plots for serum IFN-γ, TNF-α, IL-4, and IL-5 levels in α-GalCer-treated ($n = 6$) or vehicle-treated ($n = 6$) recipients at 3 h after transplantation. The plots for IFN-γ and IL-4 of vehicle-treated mice overlap with zero lines. There are statistically significant differences between the vehicle- and α-GalCer-treated groups with each cytokine (IFN-γ, TNF-α, IL-4 ($p = 0.004$), and IL-5 ($p = 0.037$)). *C*, Cytokine production from in vivo-primed and in vitro-stimulated (6 days after priming) splenocytes by α-GalCer or vehicle. Each group included three mice (each bar indicated the result from one mouse). Results are the means and SD of triplicate values. *D*, Composite box plots for serum IFN-γ, TNF-α, IL-4, and IL-5 levels in α-GalCer-treated ($n = 16$) or vehicle-treated ($n = 14$) recipients on day 5 or 6 posttransplant. There are statistically significant differences between the vehicle- and α-GalCer-treated groups with each cytokine ($p < 0.0001$). Serum from the individual mice was used to measure all four cytokines (*B–D*).

Host-residual iNKT cells are required for the prolongation of survival by adoptively transferred iNKT cells

The above observations suggest that adoptively transferred iNKT cells attenuate GVHD by affecting host-residual iNKT cells. To examine the different roles of host-residual and transferred iNKT cells more clearly, we used $J\alpha18^{-/-}$ (iNKT cell-deficient) BALB/c and C57BL/6 mice as hosts and donors, respectively.

We compared the survival time between $J\alpha18^{-/-}$ and wild-type BALB/c mice after transplantation from wild-type C57BL/6. When $J\alpha18^{-/-}$ BALB/c mice were used as recipients, the survival of these mice was significantly shorter than that of wild-type BALB/c mice after transplantation ($p = 0.017$, Fig. 4*A*). Importantly, the prolongation of survival by either the adoptive transfer of iNKT cells (Fig. 4*B*) or the administration of α-GalCer (data not shown) was not observed if the recipients were $J\alpha18^{-/-}$ BALB/c mice. Difference in the time course by α-GalCer treatment of donor $CD4^+$ T cell chimerism and the serum cytokine levels at both early phase (3–6 h) and late phase (5–6 days) posttransplant, which was seen when wild-type BALB/c mice were used as the recipients (Fig. 2, *A* and *B*), was not evident when $J\alpha18^{-/-}$ BALB/c mice were the recipients (data not shown). Surprisingly, iNKT cell administration to $J\alpha18^{-/-}$ recipient mice also did not change the levels of IFN-γ, TNF-α, IL-4, and IL-5 at 3–6 h after transplantation (Fig. 4*C*), suggesting that cytokines released after adoptive iNKT administration were produced from host-residual iNKT cells, not from infused iNKT cells.

In contrast, when $J\alpha18^{-/-}$ C57BL/6 mice were used as donors utilizing the same protocol as in the experiment shown in Fig. 1*A* (2 μg of α-GalCer or control vehicle every 4 days from the day of transplantation), the survival of the recipient BALB/c mice was prolonged by α-GalCer administration compared with vehicle administration (Fig. 4*D*), as was survival when wild-type C57BL/6 mice were used as donors (Fig. 1*A*). In this setting (donor: $J\alpha18^{-/-}$ C57BL/6), serum cytokine levels at 3–6 h posttransplant

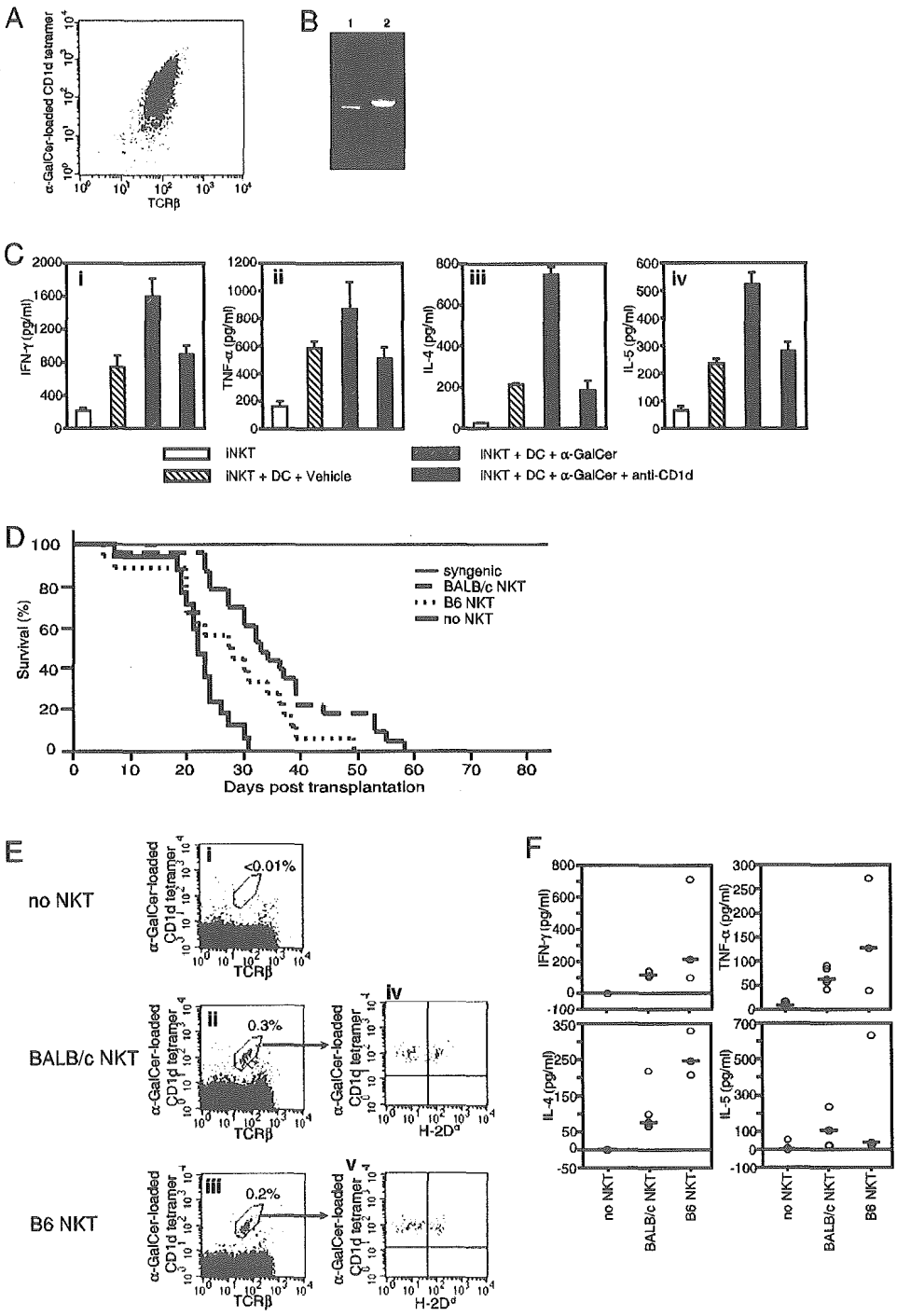

FIGURE 3. Adoptive transfer of in vitro-expanded iNKT cells. *A*, Flow cytometric analysis of in vitro-expanded iNKT cells. α-GalCer-loaded CD1d tetramer and TCRβ double-positive cells indicated iNKT cells. The purity of double-positive cells was 98%. *B*, Electrophoresed PCR products from in vitro-expanded iNKT cells using Vα14-specific 5′ primer and Cα-specific 3′ primer (*lane 1*) and those using β-actin-specific primers (*lane 2*). C, Assay for in vitro cytokine production from expanded iNKT cells stimulated by autologous splenic dendritic cells. *D*, Survival of in vitro-expanded iNKT cell-transferred recipients. Recipients receiving both C57BL/6-derived (B6 NKT, $n = 18$) and BALB/c-derived (BALB/c NKT, $n = 23$) iNKT cells survived longer than recipients without iNKT transfer (no NKT, $n = 17$) (C57BL/6-derived iNKT and no iNKT, $p = 0.016$; BALB/c-derived iNKT and no iNKT, $p < 0.0001$). The fine line represents the survival of syngeneic cell-transplanted mice (syngeneic, $n = 7$). *E*, iNKT cells in liver lymphocytes on day 6 posttransplant. α-GalCer-loaded CD1d tetramer and TCRβ double-positive cells in the liver from recipients without iNKT cell transfer (no NKT, *i*) and with the transfer of iNKT cells derived from BALB/c (BALB/c NKT, *ii*), and C57BL/6 (B6 NKT, *iii*) are shown in *left panels*. The origin of iNKT cells was evaluated by staining H-2D^d and α-GalCer-loaded CD1d tetramer (*iv* and *v*). We repeated the evaluation of liver iNKT cells seven times on day 5, 6, or 7 posttransplant. The chimerism of donor/recipient iNKT cells was not affected by the difference in the strain from which adoptively transferred iNKT cells were derived: the average difference between the two groups was as low as 8.6%, with a SD of 2.9% (range, −6 to 12%). *F*, Plots for serum IFN-γ, TNF-α, IL-4, and IL-5 levels at 3 h after transplantation from recipients without iNKT cell transfer ($n = 6$) and with the transfer of iNKT cells derived from BALB/c ($n = 5$) and C57BL/6 ($n = 3$). Horizontal lines indicate the median value. There are statistically significant differences between the "no NKT" and "BALB/c NKT" and "no NKT" and "B6 NKT" groups with each cytokine (no NKT and BALB/c NKT, $p = 0.003$ (IFN-γ, TNF-α, and IL-4) and $p = 0.008$ (IL-5); no NKT and B6 NKT, $p = 0.014$ (IFN-γ, TNF-α, and IL-4) and $p = 0.041$ (IL-5)).

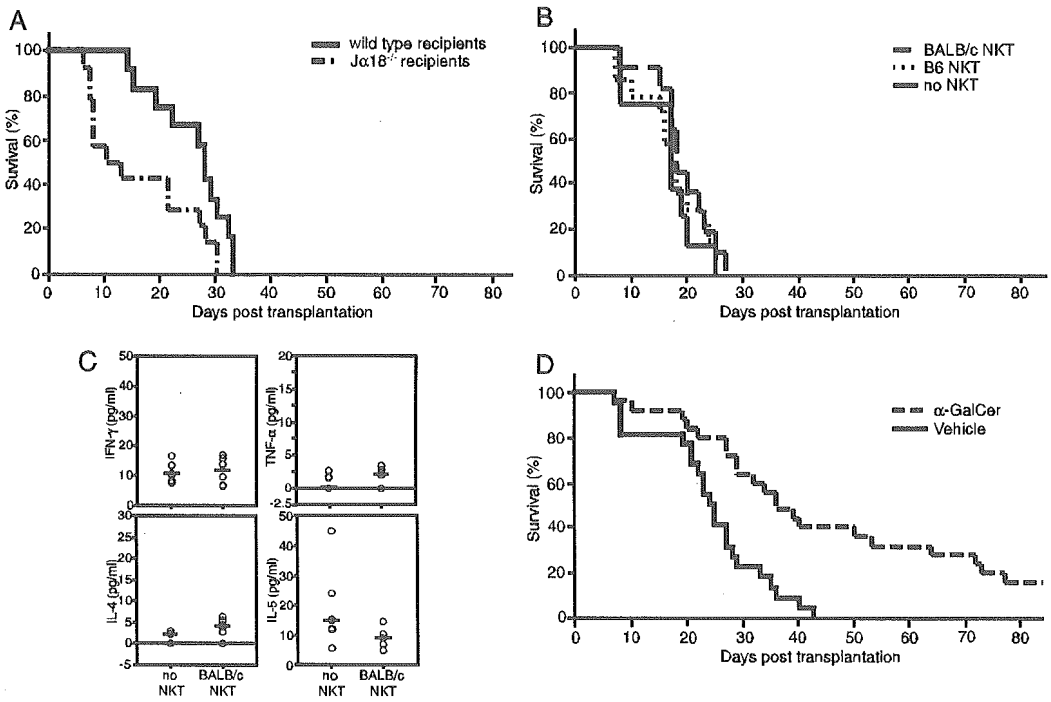

FIGURE 4. Impact of $J\alpha18^{-/-}$ mice on posttransplant survival. *A*, Wild-type ($n = 14$) recipients survived significantly longer than $J\alpha18^{-/-}$ recipients ($n = 12$) ($p = 0.017$). *B*, There was no significant difference among the survival of mice transferred with C57BL/6-derived (B6 NKT, dotted line, $n = 13$)- and BALB/c-derived (BALB/c NKT, $n = 14$) iNKT cells and without iNKT cell transfer (no NKT, $n = 9$). *C*, Plots for serum IFN-γ, TNF-α, IL-4, and IL-5 levels at 3 h after transplantation from $Ja18^{-/-}$ mice transferred with BALB/c derived ($n = 5$) or those without iNKT cell transfer ($n = 5$). Horizontal lines indicate median. *D*, Survival of α-GalCer (dashed line, $n = 25$)- and vehicle ($n = 22$)-treated mice that were transplanted with $J\alpha18^{-/-}$ donor cells. α-GalCer-treated mice survived longer than vehicle-treated mice ($p = 0.002$).

were significantly increased by α-GalCer treatment, and the serum IL-4 and IL-5 levels on 5 or 6 days posttransplant in α-GalCer-treated recipients were higher than those in vehicle-treated recipients and similar to those in wild-type recipients (data not shown).

These results collectively indicated that host-residual iNKT cells, rather than iNKT cells contained in the graft, are the major producers of various Th1 and Th2 cytokines shortly after transplant and key regulators of GVHD, and indeed are required for the regulation of GVHD by graft-contained and -adopted iNKT cells.

Combination of α-GalCer pretreatment and use of iNKT cell-depleted grafts resulted in maximal GVHD reduction and graft rejection

In experiments in which $J\alpha18^{-/-}$ C57BL/6 mice were donors, we noticed that 2 of 25 recipients treated with α-GalCer survived for >100 days, which was not the case if the wild-type C57BL/6 mice were donors (data not shown). Although this could represent a variation in the experimental conditions because there was no significant difference between the two groups, we expected that survival could be maximally improved if host-residual iNKT cells were stimulated before and after transplantation and iNKT cells were absent from the grafts. When we administered α-GalCer on days −4, 0, and 4 of transplantation and transplanted the grafts from $J\alpha18^{-/-}$ C57BL/6 mice, 8 of 17 wild-type BALB/c recipient mice survived for >100 days without obvious GVHD (Fig. 5, *A* and *B*) as expected. Without α-GalCer, there was no obvious difference in the survival of the recipients due to selection of the donor, i.e., wild-type or $J\alpha18^{-/-}$ C57BL/6 mice (cf Fig. 1*A* vs Fig. 5*A* and Fig. 1*B* vs Fig. 5*B*).

Among the eight long-term survivors described above in the setting of $J\alpha18^{-/-}$ C57BL/6 mice as donors and α-GalCer started before transplantation, seven mice completely rejected the donor cells and the remaining one mouse exhibited mixed chimerism at 6 wk posttransplant (data not shown). Therefore, we examined the time course of donor cell chimerism early after transplantation in recipients with α-GalCer that was started before transplantation. Both $Gr\text{-}1^+$ and $CD4^+$ T cells were engrafted in vehicle-treated mice (Fig. 5*C*). In contrast, both $Gr\text{-}1^+$ and $CD4^+$ T cells were rejected early after transplantation in α-GalCer-treated mice. Particularly, $Gr\text{-}1^+$ cells were never engrafted (Fig. 5*C*).

Since it is known that NK cells are major effectors in graft rejection (27) and play a role as effectors of iNKT cells in antitumor immunity by secreting IFN-γ (1, 9), we performed in vivo NK depletion by administering anti-asialo GM1 Ab. It is of note that iNKT was not depleted by this treatment (data not shown). However, the prolongation of survival (Fig. 6*A*) and graft rejection (Fig. 6*B*) by α-GalCer were still observed as seen without anti-asialo GM1 Ab. For graft rejection, therefore, some targets other than NK cells should be considered as effectors of host-residual iNKT cells activated by α-GalCer, particularly in the absence of donor iNKT cells.

Discussion

Many studies have suggested that an important physiological function of iNKT cells is to control immune responses against autoimmunity, infection, and tumors (1, 9). In transplantation immunity, iNKT cells are also thought to play a role in the induction of allograft (28–30) or xenograft tolerance (31). In this study, we examined the role of iNKT cells in GVHD mouse model systems, using an iNKT stimulator α-GalCer, adoptive transfer of in vitro-expanded iNKT cells, and $J\alpha18^{-/-}$ mice (16), and found that host-residual iNKT cells can attenuate GVHD.

Some reports have suggested that both donor bone marrow-derived (10) and host-residual (11, 12) NKT cells ($NK1.1^+$ or $DX5^+$

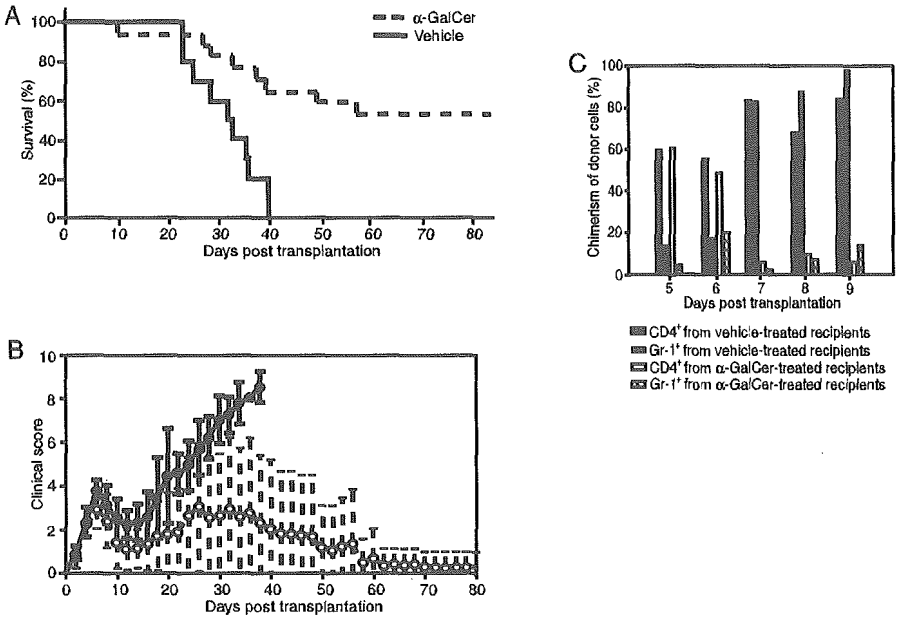

FIGURE 5. Maximal survival accompanied by graft rejection. Treatment with α-GalCer on days −4, 0, and 4 of transplantation. Survival (*A*) and clinical score (*B*, means and SD) of α-GalCer (n = 17)- and vehicle (n = 10)-treated mice that were transplanted with Jα18$^{-/-}$ donor cells. α-GalCer-treated mice lived longer (p = 0.0008). The GVHD score within the first 30 days after transplantation was significantly lower in the α-GalCer-treated group (p < 0.0001). Although the eight mice that survived for >100 days showed few signs of GVHD, they did show graft rejection or long-term mixed chimerism. *C*, Engraftment of CD4$^+$ splenocytes and Gr-1$^+$ bone marrow cells in α-GalCer- and vehicle-treated mice that were transplanted with Jα18$^{-/-}$ donor cells. The representative results of three independent and highly reproducible experiments are shown.

T cells) may suppress acute GVHD. These NKT cell populations should overlap with the iNKT cell population that we describe here. Therefore, the attenuation of GVHD by adoptive transfer of in vitro-expanded iNKT cells described here is consistent with previous results.

Recently, a report has shown that α-GalCer administration to recipients prolonged survival of GVHD mice and its administration to CD1d$^{-/-}$ mice did not prolong their survival (14). Our results show more direct evidence that such findings are caused by the functional activation of iNKT cells, with the use of Jα18$^{-/-}$ mice. Moreover, the need for host-residual iNKT cells was clearly shown by the result that adoptive iNKT cells from either strain did not attenuate GVHD if transferred to Jα18$^{-/-}$ BALB/c recipients.

Surprisingly, host-residual iNKT cells were maintained in the liver early after transplantation if C57BL/6 (donor strain)-derived iNKT cells were transferred, whereas very few host-residual iNKT cells were detected without adoptive iNKT transfer (Fig. 3*C*, *i*, *iii*, and *iv*). We could not distinguish the origin of H-2D^{d+} iNKT cells detected in the recipient liver if BALB/c strain-derived iNKT cells were transferred (Fig. 3*C*, *ii* and *iv*). It is possible that they also represent host-residual rather than injected iNKT cells. Taken together, these findings suggest that the attenuation of GVHD by adoptively transferred iNKT cells is likely to occur through the maintenance of host-residual iNKT cells, although the precise mechanism remains to be elucidated. It should also be clarified whether injected and host-residual iNKT cells locally interact with each other in a specific tissue. Particularly, it would be highly desirable if we could visualize iNKT cells in the liver by marking their strain and origin, which would be possible only after technical advances are available for the specific staining of iNKT cells. Analyzing a direct interaction of liver-isolated iNKT cells and activated MHC-mismatched iNKT cells would be of great interest, but impracticable, given the extremely low proportion of liver iNKT cells. In addition, the α-GalCer-loaded CD1d tetramer is the only tool for specifically staining iNKT cells, and the isolation procedure for iNKT cells might stimulate them and thus influence the results of in vitro analyses.

Other unexpected results include the delay in engraftment, the induction of mixed chimerism, and graft rejection by host-residual iNKT cells, particularly if α-GalCer administration was started before transplantation and Jα18$^{-/-}$ C57BL/6 mice were used as donors. This setting conferred the maximal survival benefit to the recipients because of the mildness of GVHD, albeit this occurred in our meticulous experimental mouse model. Possibly, the activated host-residual iNKT cells may suppress donor CD4$^+$ T cell function or stimulate host T cell function before total-body irradiation and transplantation. Given that mixed chimerism induces GVHD tolerance (32), host-residual iNKT cells may provide the attenuation of GVHD and the induction of mixed chimerism and graft rejection through a common mechanism that regulates graft-vs-donor immunity.

Induction of a Th2-dominant cytokine profile before the onset of obvious GVHD after transplantation (Fig. 2*B*) may, at least in part, be associated with such a mechanism, since many studies (33–35), with some conflicting reports (36, 37), have shown that Th2 cytokines protect against GVHD. In addition, some investigators have reported that IL-2, TNF-α, and IFN-γ play important roles in the development of GVHD in vivo (35, 38–41). Induction of cytokine production from residual iNKT cells by administration of α-GalCer or iNKT a few hours after transplantation was obvious. Th1 as well as Th2 cytokine secretion at the very early stage of transplantation may be favorable for balancing the recipients' and donors' T cell function and, as a result, may suppress GVHD. Besides, repeated α-GalCer administration may induce a Th2-dominant cytokine profile. These considerations, as well as previous reports that the GVHD-protective effect of NKT cells depends on IL-4 production from NKT cells (10–12, 14), support our speculation. Regarding other cytokines, several reports have noted that IL-12 (34, 42), IL-13 (43, 44), IL-15 (34, 38), and IL-18 (45) are

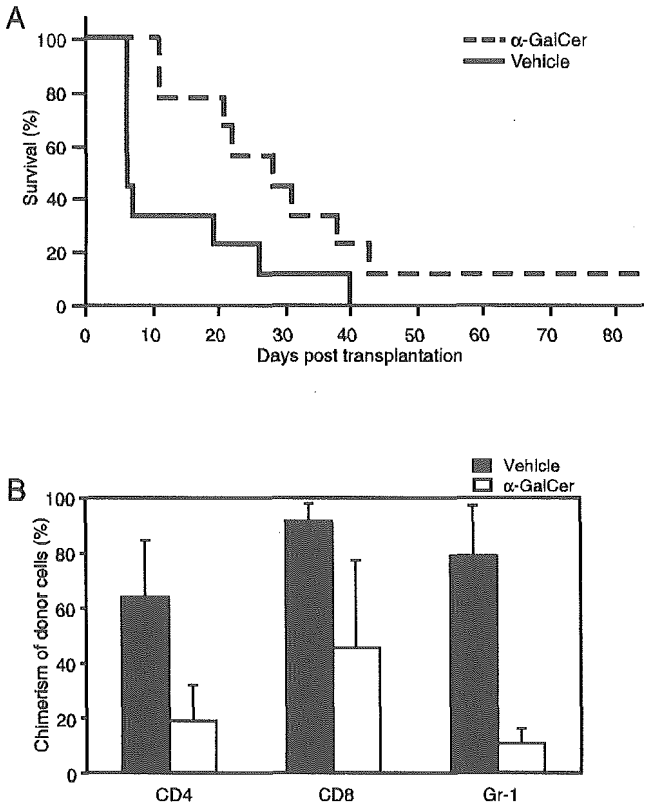

FIGURE 6. The prolongation of survival and graft rejection caused by α-GalCer treatment were unaffected by the depletion of NK cells. *A*, Survival of α-GalCer ($n = 9$)- and vehicle ($n = 9$)-treated wild-type BALB/c recipient mice. The mice were administered with anti-asialo GM1 Ab on day −1 of transplantation and transplanted with cells from wild-type C57BL/6 donor mice. α-GalCer was administered every 4 days from the day of transplantation. α-GalCer-treated mice survived longer than vehicle-treated mice ($p = 0.005$). Meantime, there was no difference between the anti-asialo GM1 Ab- and vehicle-administered groups (data not shown). *B*, Chimerism on day 7 of $CD4^+$ and $CD8^+$ splenocytes and Gr-1^+ bone marrow cells in α-GalCer and asialo GM1 Ab ($n = 6$)- and vehicle and asialo GM1 Ab ($n = 4$)-treated recipients. Asialo GM1 Ab was administered to the wild-type recipients on days −5 and −1, and α-GalCer was administered on days −4 and 0 of transplantation. Grafts were from $J\alpha18^{-/-}$ C57BL/6 mice. Significant differences were noted in each cell type ($CD4^+$, $p = 0.002$; $CD8^+$ and Gr-1^+, $p < 0.0001$).

also associated with GVHD. However, we could not obtain sufficient samples from sick mice to measure such various cytokines simultaneously. Although we were unable to evaluate all of these cytokines in this study, we hope we will be able to analyze a complete set of cytokines in future studies.

To further complicate this scenario, our findings also revealed that the absence of iNKT cells in the graft enhances the suppression of engraftment of donor cells. A simple interpretation of this result is that iNKT cells in the graft help donor cells engraft, which is apparently opposite to the effect of host-residual iNKT cells. While attenuating GVHD by inducing host-residual iNKT cells, graft-contaminated iNKT cells may suppress host-vs-graft immunity. We observed a delay of engraftment when we adoptively transferred iNKT cells expanded from the BALB/c strain while transplanting grafts from $J\alpha18^{-/-}$ C57BL/6 mice (data not shown). Furthermore, we observed high levels of serum cytokines after transplantation and in vitro-expanded iNKT cells only when recipients had iNKT cells. Therefore, these functional differences may simply depend on the place, tissue-residual iNKT cells or blood-borne iNKT cells that are pre-expanded in vitro. Under physiological conditions, the cytokine status could be created by iNKT cells in the liver to prevent autoreactivity, and this environment may be able to prevent GVHD and influence incoming iNKT cells to prevent the attack of the donor graft by the recipient lymphocytes. Alternatively, the suppression of graft-vs-host immunity by host-residual iNKT cells and the suppression of host-vs-graft immunity by graft-contaminated iNKT cells could also be explained by the recognition of non-self through members of Ly49 (46–48). At least NK cells, which were generally recognized as major effectors in graft rejection, are not the downstream effectors of iNKT cell-dependent graft rejection.

In the clinical setting, there is increasing interest in the kinetics of the establishment of donor chimerism because of the development of reduced intensity conditioning regimens for allogeneic stem cell transplantation. Our results suggest that recipient-residual iNKT cells play a role against the establishment of donor chimerism as well as in the prevention of GVHD. Warn us that α-GalCer must be used carefully to prevent or treat GVHD are the facts that the combination of overstimulation of recipient iNKT cells before transplantation and that the lack of iNKT cells in grafts can cause graft rejection.

In conclusion, host-residual iNKT cells have a regulatory function in GVHD. α-GalCer therapy has already been performed in clinical trials in cancer patients and was well tolerated (49). It may be attractive to use α-GalCer or iNKT cells therapeutically for the prevention or treatment of GVHD. However, care must be taken in its clinical application because of the possibility that the activation of host-residual iNKT cells could also increase graft rejection.

Acknowledgments

We thank M. Kronenberg (La Jolla Institute for Allergy and Immunology, La Jolla, CA) for agreeing to provide us with α-GalCer-loaded murine CD1d tetramer. We thank M. Harada (Chiba University, Chiba, Japan) for preparing $J\alpha18^{-/-}$ mice, T. Nakayama (Chiba University) for providing the Sf9 cell line and baculovirus-expressing mouse CD1d/β_2-microgloblin, and T. Ito (Chiba University) for considerable advice on the production of α-GalCer-loaded CD1d tetramers. We also thank E. Nagata and Y. Sato for providing excellent technical assistance.

Disclosures

The authors have no financial conflict of interest.

References

1. Godfrey, D., K. Hammond, L. Poulton, and A. Baxter. 2000. NKT cells: Facts, functions and fallacies. *Immunol. Today* 21: 573–583.
2. Wilson, M. T., A. K. Singh, and L. Kaer. 2002. Immunotherapy with ligands of natural killer T cells. *Trends Mol. Med.* 8: 225–231.
3. Fowlkes, B., A. Kruisbeek, H. Ton-That, M. Weston, J. Coligan, R. Schwartz, and D. Pardoll. 1987. A novel population of T cell receptor αβ-bearing thymocytes which predominantly express a single vβ8 gene family. *Nature* 329: 251–254.
4. Budd, R., G. Miescher, R. Howe, R. Lees, C. Bron, and H. MacDonald. 1987. Developmentally regulated expression of T cell receptor β chain variable domain is immature thymocytes. *J. Exp. Med.* 166: 577–582.
5. Dellabona, P., E. Padovan, G. Casorati, M. Brockhaus, and A. Lanzavecchia. 1994. An invariant Vα24-JαQ/Vβ11 T cell receptor is expressed in all individuals by clonally expanded $CD4^-CD8^-$ cells. *J. Exp. Med.* 180: 1171–1176.
6. Porcelli, S., D. Gerdes, A. Fertig, and S. Balk. 1996. Human T cells expressing an invariant Vα24-JαQ TCRα are $CD4^-$ and heterogenous with respect to TCRβ expression. *Hum. Immunol.* 48: 63–67.
7. Lantz, O., and A. Bendelac. 1994. An invariant T cell receptor α chain is used by a unique subset of major histocompatibility complex class I-specific $CD4^+$ and $CD4^-8^-$ T cells in mice and humans. *J. Exp. Med.* 180: 1097–1106.
8. Taniguchi, M., M. Harada, S. Kojo, T. Nakayama, and H. Wakao. 2003. The regulatory role of Vα14 NKT cells in innate and acquired immune response. *Annu. Rev. Immunol.* 21: 483–513.
9. Joyce, S. 2001. CD1d and natural T cells: How their properties jump-start the immune system. *Cell Mol. Life Sci.* 58: 442–469.
10. Zeng, D., D. Lewis, S. Dejbakhsh-Jones, F. Lan, M. Garcia-Ojeda, R. Sibley, and S. Strober. 1999. Bone marrow $NK1.1^-$ and $NK1.1^+$ T cells reciprocally regulate acute versus host disease. *J. Exp. Med.* 189: 1073–1081.

11. Lan, F., D. Zeng, M. Higuchi, P. Huie, J. P. Higgins, and S. Strober. 2001. Predominance of NK1.1$^+$TCR$\alpha\beta^+$ or DX5$^+$TCR$\alpha\beta^+$ T cells in mice conditioned with fractionated lymphoid irradiation protects against graft-versus-host disease: "natural suppressor" cells. *J. Immunol.* 167: 2087–2096.
12. Lan, F., D. Zeng, M. Higuchi, J. P. Higgins, and S. Strober. 2003. Host conditioning with total lymphoid irradiation and antithymocyte globulin prevents graft-versus-host disease: the role of CD1-reactive natural killer T cells. *Biol. Blood Marrow Transplant* 9: 355–363.
13. Morecki, S., S. Panigrahi, G. Pizov, E. Yacovlev, Y. Gelfand, O. Eizik, and S. Slavin. 2004. Effect of KRN7000 on induced graft-vs-host disease. *Exp. Hematol.* 32: 630–637.
14. Hashimoto, D., S. Asakura, S. Miyake, T. Yamamura, L. Van Kaer, C. Liu, M. Tanimoto, and T. Teshima. 2005. Stimulation of host NKT cells by synthetic glycolipid regulates acute graft-versus-host disease by inducing Th2 polarization of donor t cells. *J. Immunol.* 174: 551–556.
15. Haraguchi, K., T. Takahashi, K. Hiruma, Y. Kanda, Y. Tanaka, S. Ogawa, S. Chiba, O. Miura, H. Sakamaki, and H. Hirai. 2004. Recovery of Vα24$^+$ NKT cells after hematopoietic stem cell transplantation. *Bone Marrow Transplant* 34: 595–602.
16. Cui, J., T. Shin, T. Kawano, H. Sato, E. Kondo, I. Toura, Y. Kaneko, K. H., M. Kanno, and M. Taniguchi. 1997. Requirement for Vα14 NKT cells in IL-12-mediated rejection of tumors. *Science* 278: 1623–1626.
17. Matsuda, J. L., O. V. Naidenko, L. Gapin, T. Nakayama, M. Taniguchi, C.-R. Wang, Y. Koezuka, and M. Kronenberg. 2000. Tracking the response of natural killer T cells to a glycolipid antigen using CD1d tetramers. *J. Exp. Med.* 192: 741–754.
18. Smyth, M. J., N. Y. Crowe, D. G. Pellicci, K. Kyparissoudis, J. M. Kelly, K. Takeda, H. Yagita, and D. I. Godfrey. 2002. Sequential production of interferon-γ by NK1.1$^+$ T cells and natural killer cells is essential for the antimetastatic effect of α-galactosylceramide. *Blood* 99: 1259–1266.
19. Sharif, S., G. A. Arreaza, P. Zucker, Q.-S. Mi, J. *Sondhi*, O. V. Naidenko, M. Kronenberg, Y. Koezuka, T. L. Delovitch, J.-M. Gombert, et al. 2001. Activation of natural killer T cells by α-galactosylceramide treatment prevents the onset and recurrence of autoimmune type 1 diabetes. *Nat. Med.* 7: 1057.
20. Nakagawa, R., I. Nagafune, Y. Tazunoki, H. Ehara, H. Tomura, R. Iijima, K. Motoki, M. Kamishohara, and S. Seki. 2001. Mechanisms of the antimetastatic effect in liver and of the hepatocyte injury induced by α-galactosylceramide in mice. *J. Immunol.* 166: 6578–6584.
21. Chiodoni, C., A. Stoppacciaro, S. Sangaletti, G. Gri, B. Cappetti, Y. Koezuka, and Mario P. Colombo. 2001. Different requirements for α-galactosylceramide and rIL-12 antitumor activity in the treatment of C-26 colon carcinoma hepatic metastases. *Eur. J. Immunol.* 31: 3101–3110.
22. Cooke, K., L. Kobzik, T. Martin, J. Brewer, J. J. Delmonte, J. Crawford, and J. Ferrara. 1996. An experimental model of idiopathic pneumonia syndrome after bone marrow transplantation: I. The roles of minor H antigens and endotoxin. *Blood* 88: 3230–3239.
23. Singh, N., S. Hong, D. C. Scherer, I. Serizawa, N. Burdin, M. Kronenberg, Y. Koezuka, and L. Van Kaer. 1999. Cutting edge: Activation of NK T cells by CD1d and α-galactosylceramide directs conventional T cells to the acquisition of a Th2 phenotype. *J. Immunol.* 163: 2373–2377.
24. Chamoto, K., T. Takeshima, A. Kosaka, T. Tsuji, J. Matsuzaki, Y. Togashi, H. Ikeda, and T. Nishimura. 2004. NKT cells act as regulatory cells rather than killer cells during activation of NK cell-mediated cytotoxicity by α-galactosylceramide in vivo. *Immunol. Lett.* 95: 5–11.
25. Kaer, L. V. 2005. α-galactosylceramide therapy for autoimmune diseases: Prospects and obstacles. *Nat. Rev. Immunol.* 5: 31–42.
26. Burdin, N., L. Brossay, and M. Kronenberg. 1999. Immunization with α-galactosylceramide polarizes CD1-reactive NK T cells towards Th2 cytokine synthesis. *Eur. J. Immunol.* 29: 2014–2025.
27. Barao, I., and W. Murphy. 2003. The immunobiology of natural killer cells and bone marrow allograft rejection. *Biol. Blood Marrow Transplant* 9: 727–741.
28. Seino, K., K. Fukao, K. Muramoto, K. Yanagisawa, Y. Takada, S. Kakuta, Y. Iwakura, L. Kaer, K. Takeda, T. Nakayama, et al. 2001. Requirement for natural killer T (NKT) cells in the induction of allograft tolerance. *Proc. Natl. Acad. Sci. USA* 98: 2577–2581.
29. Chargui, J., T. Hase, S. Wada, T. Naganuma, and R. Yoshimura. 2001. NKT cells **as nonspecific immune-regulator inducing tolerance in mouse model transplan**tation. *Transplant. Proc.* 33: 3833–3834.
30. Higuchi, M., D. Zeng, J. Shizuru, J. Gworek, S. Dejbakhsh-Jones, M. Taniguchi, and S. Strober. 2002. Immune tolerance to combined organ and bone marrow transplants after fractionated lymphoid irradiation involves regulatory NK T cells and clonal deletion. *J. Immunol.* 169: 5564–5570.
31. Ikehara, Y., Y. Yasunami, S. Kodama, T. Maki, M. Nkano, T. Nakayama, M. Taniguchi, and S. Ikeda. 2000. CD4$^+$ 1 Vα24 natural killer T cells are essential for acceptance of rat islet xenografts in mice. *J. Clin. Invest.* 105: 1761–1767.
32. Kolb, H.-J., C. Schmid, X. Chen, A. Woiciechowski, M. Roskrow, M. Weber, W. Guenther, G. Ledderose, and M. Schleuning. 2003. Adoptive immunotherapy in chimeras with donor lymphocytes. *Acta Haematol.* 110: 110–120.
33. Fowler, D. H., and R. E. Gress. 2000. Th2 and Tc2 cells in the regulation of GVHD, GVL, and graft rejection: considerations for the allogeneic transplantation therapy of leukemia and lymphoma. *Leuk. Lymphoma* 38: 221–234.
34. Teshima, T., and J. Ferrara. 2002. Understanding the alloresponse: new approaches to graft-versus-host disease prevention. *Semin. Hematol.* 39: 15–22.
35. Goker, H., I. C. Haznedaroglu, and N. J. Chao. 2001. Acute graft-vs-host disease: pathobiology and management. *Exp. Hematol.* 29: 259–277.
36. Murphy, W. J., L. A. Welniak, D. D. Taub, R. H. Wiltrout, P. A. Taylor, D. A. Vallera, M. Kopf, H. Young, D. L. Longo, and B. R. Blazar. 1998. Differential effects of the absence of interferon-γ and IL-4 in acute graft-versus-host disease after allogeneic bone marrow transplantation in mice. *J. Clin. Invest.* 102: 1742–1748.
37. Nikolic, B., S. Lee, R. T. Bronson, M. J. Grusby, and M. Sykes. 2000. Th1 and Th2 mediate acute graft-versus-host disease, each with distinct end-organ targets. *J. Clin. Invest.* 105: 1289–1298.
38. Reddy, P., and J. L. M. Ferrara. 2003. Immunobiology of acute graft-versus-host disease. *Blood Rev.* 17: 187–194.
39. Shalaby, M. R., B. Fendly, K. C. Sheehan, R. D. Schreiber, and A. J. Ammann. 1989. Prevention of the graft-versus-host reaction in newborn mice by antibodies to tumor necrosis factor-α. *Transplantation* 47: 1057–1061.
40. Via, C. S., and F. D. Finkelman. 1993. Critical role of interleukin-2 in the development of acute graft-versus-host disease. *Int. Immunol.* 5: 565–572.
41. Mowat, A. 1989. *Antibodies to IFN-γ prevent immunologically mediated intes*tinal damage in murine graft-versus-host reaction. *Immunology* 68: 18–23.
42. Deeg, H. J. 2001. Cytokines in graft-versus-host disease and the graft-versus-leukemia reaction. *Int. J. Hematol.* 74: 26–32.
43. Jordan, W. J., P. A. Brookes, R. M. Szydlo, J. M. Goldman, R. I. Lechler, and M. A. Ritter. 2004. IL-13 production by donor T cells is prognostic of acute graft-versus-host disease following unrelated donor stem cell transplantation. *Blood* 103: 717–724.
44. Imamura, M., Y. Tsutsumi, Y. Miura, T. Toubai, and J. Tanaka. 2003. Immune reconstitution and tolerance after allogeneic hematopoietic stem cell transplantation. *Hematology* 8: 19–21.
45. Holler, E. 2002. Cytokines, viruses, and graft-versus-host disease. *Curr. Opin. Hematol.* 9: 479–484.
46. Maeda, M., S. Lohwasser, T. Yamamura, and F. Takei. 2001. Regulation of NKT cells by Ly49: Analysis of primary NKT cells and generation of NKT cell line. *J. Immunol.* 167: 4180–4186.
47. Ikarashi, Y., R. Mikami, A. Bendelac, M. Terme, N. Chaput, M. Terada, T. Tursz, E. Angevin, F. A. Lemonnier, H. Wakasugi, and L. Zitvogel. 2001. Dendritic cell maturation overrules H-2D-mediated natural killer T (NKT) cell inhibition: Critical role for B7 in CD1d-dependent NKT cell interferon γ production. *J. Exp. Med.* 194: 1179–1186.
48. Hayakawa, Y., S. Berzins, N. Crowe, D. Godfrey, and M. Smyth. 2004. Antigen-induced tolerance by intrathymic modulation of self-recognizing inhibitory receptors. *Nat. Immunol.* 5: 590–596.
49. Giaccone, G., C. J. A. Punt, Y. Ando, R. Ruijter, N. Nishi, M. Peters, B. M. E. von Blomberg, R. J. Scheper, H. J. J. van der Vliet, A. J. M. van den Eertwegh, et al. 2002. A Phase I study of the natural killer T-cell ligand α-galactosylceramide (KRN7000) in patients with solid tumors. *Clin. Cancer Res.* 8: 3702–3709.

Table 1 Patient clinical features

Clinical features	*Diagnosis (November 1998)*	*Disease progression (November 2001)*	*Disease recurrence (February 2004)*	*B hepatitis onset (September 2004)*
Rai clinical stage	I	II	II	0
CD38	Negative	Negative	Negative	Negative
Zap 70	Positive	Positive	Positive	Negative
CD4/CD8	0.95	0.90	0.85	0.80
Beta 2 microglobulin (mcg/l)	1503	1825	1844	1325
Serum Ig level (g/l)	0.980	0.790	0.660	0.620
HBsAg	Negative	Negative	Negative	Negative
HBsAb	Negative	Negative	Negative	Negative
HBcAb	Positive	Positive	Positive	Positive
HBeAg	Negative	Negative	Negative	Positive
HBeAb	Positive	Positive	Positive	Positive
HBV DNA	NA	NA	NA	200.000/μl

Ig: immunoglobulin.

followed up until about 2 years later (February 2004) when, for a disease recurrence, rituximab was given again.

At this time, all the above hepatitis markers remained unmodified. After four weekly standard doses of rituximab a GPR was recorded, and then six monthly courses (150 mg/m^2) of the same agent were administered as maintenance therapy. In September 2004, being the patient in CR, he was admitted with acute hepatitis. HBV DNA strains (200 000 copies/ml) were detected, whereas the HbsAg-negative status persisted.

Under antiviral treatment with lamivudine, the viraemia decreased to 3300 copies/ml within 2 weeks. Nevertheless, hepatic function did not recover, and the patient died 32 days after his admission.

Although reactivation of HBV in HBsAg-positive patients is a well-documented complication of cytotoxic treatments,[4,5] to the best of our knowledge, this is the first case of HBV reactivation in a B-CLL patient after rituximab. Moreover, we recorded the presence of HBcAb and HBeAb associated with the negativity of HbsAg and HBsAb, indicating that these findings are a long-lasting occult infection of a HBV variant strain. Given the high efficacy of prophylaxis with lamivudine, testing HBV DNA before immunosuppressive and cytotoxic treatments, including the anti-CD20 antibodies, should be recommended in order to identify HBV carriers among patients presenting HBcAb alone without any other serological HBV markers, since HBsAg routine tests may be unreliable in S-gene mutated variants.

P Niscola[1]
MI Del Principe[1]
L Maurillo[1]
A Venditti[1]
F Buccisano[1]
D Piccioni[1]
S Amadori[1]
G Del Poeta[1]

[1]*Department of Hematology, Tor Vergata University, Rome, Italy*

References

1 Dervite I, Hober D, Morel P. Acute hepatitis B in a patient with antibodies to hepatitis B surface antigen who was receiving rituximab. *N Engl J Med* 2001; **344**: 68–69.
2 Westhoff TH, Jochimsen F, Schmittel A, Stoffler-Meilicke M, Schafer JH, Zidek W *et al.* Fatal hepatitis B virus reactivation by an escape mutant following rituximab therapy. *Blood* 2003; **102**: 1930.
3 Ng HJ, Lim LC. Fulminant hepatitis B virus reactivation with concomitant listeriosis after fludarabine and rituximab therapy: case report. *Ann Hematol* 2001; **80**: 549–552.
4 Picardi M, Pane F, Quintarelli C, De Renzo A, Del Giudice A, De Divitiis B *et al.* Hepatitis B virus reactivation after fludarabine-based regimens for indolent non-Hodgkin's lymphomas: high prevalence of acquired viral genomic mutations. *Haematologica* 2003; **88**: 1296–1303.
5 Tsutsumi Y, Tanaka J, Kawamura T, Miura T, Kanamori H, Obara S *et al.* Possible efficacy of lamivudine treatment to prevent hepatitis B virus reactivation due to rituximab therapy in a patient with non-Hodgkin's lymphoma. *Ann Hematol* 2004; **83**: 58–60.

Mutations of the Notch1 gene in T-cell acute lymphoblastic leukemia: analysis in adults and children

Leukemia (2005) **19**, 1841–1843. doi:10.1038/sj.leu.2403896; published online 4 August 2005

TO THE EDITOR

Notch signaling plays a key role in the cell fate decision at various differentiation branch points.[1] In mammals, it has been well recognized that the deregulated activation of Notch signaling leads to tumor development.[2] This concept is highlighted by a recent report demonstrating that as much as 60% of childhood T-cell acute lymphoblastic leukemia (T-ALL) has mutations in the *Notch1* gene.[3] The resulting amino-acid changes have been found in the heterodimerization (HD) domains at the C- and N-termini of the extracellular and transmembrane subunits (HD^{EC} and HD^{TM} domains), respectively, and the transcriptional activation (TA) and PEST domains at the cytoplasmic region of the transmembrane subunit. The former mutations are thought to reduce the affinity between the two subunits, which subsequently leads to ligand-independent γ-cleavage of the Notch1 transmembrane subunit and production of an activated Notch1 intracellular domain. In the latter, insertion or deletion mutations introduce a premature stop codon that results in truncation of the PEST domain, which

Correspondence: Dr S Chiba, Department of Cell Therapy and Transplantation Medicine, University of Tokyo Hospital, 7-3-1 Hongo, Bunkyo-ku, Tokyo 113-8655, Japan; Fax: +81 3 5689 7286; E-mail: schiba-tky@umin.ac.jp
Received 13 June 2005; accepted 28 June 2005; published online 4 August 2005

eventually causes prolonged half-life of the cleaved Notch1 intracellular domain. Both mutations appear to result in activation of Notch signaling and initiate or develop leukemia.[3] Extremely high frequency of activating mutations of the *Notch1* gene gave us an idea that T-ALL is commonly dependent on abnormal Notch1 activation. Based on these findings, it has been postulated that γ-secretase inhibitors, which are considered as a treatment modality against Alzheimer's disease,[4] could be useful as anti-T-ALL drugs.

While adult T-ALL has pathological characteristics common to childhood T-ALL, some differences have been recognized from both clinical observations[5] and molecular studies.[6] Therefore, it would be worthwhile to examine *Notch1* mutations in adult T-ALL to gain insight into the entity and subclassification of T-ALL, based on the knowledge of exceptionally high frequency of *Notch1* mutations in childhood T-ALL.

In the current study, we found that *Notch1* mutations were frequent in both adult and childhood T-ALLs. In the 14 adult T-ALL samples, we found an in-frame 3-nucleotide deletion mutation in one and an in-frame 3-nucleotide insertion mutation in another in the HD^{EC} domain. The former was described in the previous report as one of the 'hot spots' that leads to the deletion of 1579V. In the latter (Figure 1, upper panel), Gly was inserted between amino-acids 1597L and 1598S. Although the same mutation was not described in the previous report, these two residues are conserved among the vertebrate *Notch1* gene products, and thus 1598 Ins G may also cause ligand-independent activation of Notch1. In the HD^{TM} domain, we found a missense mutation 1681I/N in one case, which was described in children (Figure 1, middle panel). In the TA domain, there was a mutation with a 3-nucleotide deletion and a 4-nucleotide insertion at the same position, resulting in a frame shift and a premature stop codon (Figure 1, lower panel). In the PEST domain, there was a mutation with a 5-nucleotide insertion, also resulting in a premature termination of translation. Both of these insertion mutations lead to truncation of the PEST domain.

Overall, we found five potentially activating mutations in five adult patients, among 14, with ages of 17, 19, 24, 31 and 37 years (summarized in Table 1). No sample showed mutations at both the HD and PEST domains, most likely because of the small sample number.

In 10 out of the 14 adults analyzed, we previously studied the deletion of *CDKN2A* antioncogene. Although homozygous deletion of this gene, which is known to be frequent in childhood T-ALL, was found in only one of these 10 cases,[7] we also found an activating *Notch1* mutation in the HD domain in the same sample. From this observation, we can conclude that activating mutation of *Notch1* gene and inactivation of *CDKN2A* gene, which are the most frequent abnormalities in T-ALL, are not likely to be mutually exclusive.

We also analyzed the *Notch1* gene in 33 childhood T-ALL samples. We found 12, 3 and 2 mutations in the HD^{EC}, HD^{TM}

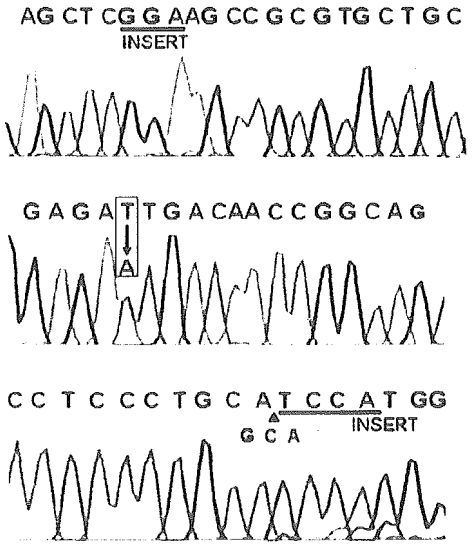

Figure 1 Sequence analysis of adult T-ALL patients. (upper panel) Insertion at 4792, GGA (HD^{EC} domain); (middle panel) missense mutation at 5042, T→A (HD^{TM} domain); (lower panel) deletion at 7032, GCA, and insertion at the same position, TCCA.

Table 1 Notch1 heterodimerization domain and PEST domain mutational status and deletion of *CDKN2A* gene in primary T-ALL cells from adult patients

ID	*Age (years)*	*CDKN2A*	*Notch1*	*Seq HD domain*	*Mut HD domain*	*Seq PEST domain*	*Mut PEST domain*
T-ALL 1	20	+/+	WT	SNP 5097 C/T	—	—	—
T-ALL 2	31	+/+	**Mut**	**{5042 T/A** SNP 5097 C/T}	**1681 I/N**	—	—
T-ALL 3	18	+/+	WT	SNP 5097 C/T	—	—	—
T-ALL 4	72	+/+	WT	SNP 5097 C/T	—	—	—
T-ALL 5	19	+/+	**Mut**	SNP 5097 C/T	—	**Ins. 7374 ATTCT**	**2458 LFCPRRAPPCPRRCHPRWSHPStop**
T-ALL 6	19	+/+	WT	SNP 5097 C/T	—	—	—
T-ALL 7	24	+/+	**Mut**	SNP 5097 C/T	—	**{Del. 7032 GCA Ins. 7035 TCCA}**	**2344 HPWHGRPAAQStop**
T-ALL 8	17	−/−	**Mut**	**{Ins. 4792 GGA** SNP 5097 C/T}	**1598 Ins. G**	—	—
T-ALL 9	42	+/+	WT	SNP 5097 C/T	—	—	—
T-ALL 10	68	+/+	WT	SNP 5097 C/T	—	—	—
T-ALL 11	65	ND	WT	SNP 5097 C/T	—	—	—
T-ALL 12	37	ND	**Mut**	**{Del. 4735 GTG** SNP 5097 C/T}	**1579 Del. V**	—	—
T-ALL 13	17	ND	WT	—	—	—	—
T-ALL 14	55	ND	WT	SNP 5097 C/T	—	—	—

Seq = sequence; HD = heterodimerization domain; Mut = mutation; WT = wild-type; Ins = insertion; Del = deletion; +/+, no deletion; −/−, homozygous deletion; ND = not determined.
Bold indicate samples which have a mutation.